

University of Southern Queensland  
Faculty of Engineering & Surveying

**INVESTIGATION OF THE FLEXURAL  
STRENGTHENING OF CONCRETE BEAMS USING  
EXTERNAL PRESTRESSING**

A dissertation submitted by

Mr Shawn Wayne Davis

in fulfilment of the requirements of

**ENG4112 Research Project**

towards the degree of

**Bachelor of Engineering (Civil)**

Submitted: October, 2005

# Abstract

External prestressing offers a viable strengthening and rehabilitation tool for aging, overloaded or weakening members. This technology can therefore help to strengthen all existing flexural members that external prestressing can practically be applied to, including bridge girders and structural flexural beams. This project aims to investigate the variation in flexural strength of rectangular reinforced concrete beams with the application of an external prestress. The project aims at comparing the deflection and crack patterns of two loading systems along with the flexural capacity increase. These 2 loading conditions can hopefully represent or model the loading patterns that such flexural members will experience in service. With the inclusion of the external prestressing, not only will the flexural strength be expected to increase, but the deflection decrease, and crack widths minimised.

Some major aims of the project are as follows:

- To obtain the magnitude of the change in the specimens flexural strength after prestressing.
- To observe and compare the change in the specimens deflections and crack widths.

Four test specimens were prepared and cured in a similar environment. Two of the beams were used as control beams, and two of the beams were given an external prestress. The displacement and flexural loading capacity of the test beams were compared to the control beams for the two loading positions.

The results have shown that under both loading positions, the reinforced concrete beams have reacted with positive results. The first test involving the loading position

---

of  $A = 1$  m, achieved a 50% increase in flexural strength. The deflection of the prestressed beam was reduced by 63.18% after prestressing was applied. For the second test with the loading position of  $A = 0.5$  m, a 74% increase in flexural strength was achieved with a 59% deflection reduction after prestress.

The large increase in flexural strength and effectiveness of the prestressing force to close the cracks present within the beam reinforce the effectiveness of this technique as a means to rehabilitate flexural members in service. Though this prestressing method is a more “conventional” method, the experimental data and results further prove that it is in-fact an effective method.

All these advantages make this classical style post-tensioning method effective in the rehabilitation or strengthening of Australia’s concrete structures. Hopefully the project will show positive results and lead to further studies and applications of the external prestressing technology for flexural strengthening.

The second order effects of the prestressing effect have not been included, where at mid-span the depth of the prestressing bar varies with load applied, as the beam deflects. The effects have been assumed negligible for loads used in this study, but for increasing loads, or increasing sensitive members, these effects should be taken into account.

University of Southern Queensland  
Faculty of Engineering and Surveying

<b>ENG4111/2 <i>Research Project</i></b>
--

### **Limitations of Use**

The Council of the University of Southern Queensland, its Faculty of Engineering and Surveying, and the staff of the University of Southern Queensland, do not accept any responsibility for the truth, accuracy or completeness of material contained within or associated with this dissertation.

Persons using all or any part of this material do so at their own risk, and not at the risk of the Council of the University of Southern Queensland, its Faculty of Engineering and Surveying or the staff of the University of Southern Queensland.

This dissertation reports an educational exercise and has no purpose or validity beyond this exercise. The sole purpose of the course pair entitled “Research Project” is to contribute to the overall education within the student’s chosen degree program. This document, the associated hardware, software, drawings, and other material set out in the associated appendices should not be used for any other purpose: if they are so used, it is entirely at the risk of the user.

**Prof G Baker**

Dean

Faculty of Engineering and Surveying

# Certification of Dissertation

I certify that the ideas, designs and experimental work, results, analyses and conclusions set out in this dissertation are entirely my own effort, except where otherwise indicated and acknowledged.

I further certify that the work is original and has not been previously submitted for assessment in any other course or institution, except where specifically stated.

MR SHAWN WAYNE DAVIS

Q11215594

---

Signature

---

Date

# Acknowledgments

This research was carried out under the principal supervision of Dr Thiru Aravinthan, whom I would like to thank for all his guidance and support. I would also like to give a special thanks to T.G.Suntharauadivel who helped with the project specimen preparation testing phase and Steven Luther for his assistance in this project.

MR SHAWN WAYNE DAVIS

*University of Southern Queensland*

*October 2005*

# Contents

<b>Abstract</b>	<b>i</b>
<b>Acknowledgments</b>	<b>v</b>
<b>List of Figures</b>	<b>ix</b>
<b>List of Tables</b>	<b>xii</b>
<b>Chapter 1 Introduction</b>	<b>1</b>
1.1 General Background . . . . .	1
1.2 Research Aim and Objectives . . . . .	3
1.3 External Prestress . . . . .	4
1.4 Dissertation Overview . . . . .	6
1.5 Summary . . . . .	7
<b>Chapter 2 Review of External Prestressing</b>	<b>8</b>
2.1 Introduction . . . . .	8
2.2 Historical Development . . . . .	9

<b>CONTENTS</b>	<b>vii</b>
2.3 Previous Studies . . . . .	10
<b>Chapter 3 Specimen Design</b>	<b>12</b>
3.1 Introduction . . . . .	12
3.2 Specimen Design Approach . . . . .	12
3.3 Beam Specimen Design . . . . .	15
3.3.1 Beam Dimensions . . . . .	16
3.3.2 Steel Reinforcement . . . . .	17
3.4 Control Condition Strength Capacity . . . . .	19
3.5 Prestress Design . . . . .	26
3.6 Prestressed Strength Capacity . . . . .	29
<b>Chapter 4 Experimental Methodology</b>	<b>33</b>
4.1 Introduction . . . . .	33
4.2 Experimental Procedure and Variables . . . . .	34
4.3 Formwork Construction and Details . . . . .	35
4.4 Steel Reinforcement Details . . . . .	37
4.5 Concreting . . . . .	40
4.6 Instrumentation . . . . .	43
4.6.1 Strain Gauge placement . . . . .	44
4.6.2 Linear Variable Displacement Transducer (LVDT) Placement . . . . .	47



<b>CONTENTS</b>	<b>viii</b>
4.6.3 Load Cells and Anchorage Apparatus . . . . .	47
<b>Chapter 5 Results and Discussion</b>	<b>52</b>
5.1 Introduction . . . . .	52
5.1.1 Compression Testing Results . . . . .	54
5.1.2 Flexural testing of Control Beams . . . . .	55
5.1.3 Flexural testing of Prestressed Beams . . . . .	58
5.1.4 Control Beams versus Prestressed Beams . . . . .	62
5.2 Comparison of Loading Position . . . . .	64
5.3 Theoretical versus Experimental Results . . . . .	68
5.4 Increases in Prestressing Force . . . . .	70
5.5 Conclusion . . . . .	74
<b>Chapter 6 Conclusion</b>	<b>75</b>
6.1 Completion of Aims and Objectives . . . . .	75
6.2 Conclusion . . . . .	77
6.3 Recommendations for further studies . . . . .	77
<b>References</b>	<b>79</b>
<b>Appendix A Project Specification</b>	<b>80</b>

# List of Figures

3.1	Loading Position Arrangement for Test Beams . . . . .	13
3.2	Bending Moment Diagram at $A = 1$ m . . . . .	14
3.3	Bending Moment Diagram at $A = 0.5$ m . . . . .	14
3.4	Shear Force Diagram . . . . .	15
3.5	Front View of Design Specimen . . . . .	16
3.6	Top View of Beam Specimen . . . . .	16
3.7	Typical Cross-Section of Beam Specimen . . . . .	17
3.8	Shear Reinforcing Spacing . . . . .	18
3.9	Typical Section Reinforcing . . . . .	18
3.10	Mid-Span Section Flexural Analysis . . . . .	19
3.11	Strain Diagram . . . . .	22
3.12	Cross Section of the Anchorage Plates and Prestressing Bars . . . . .	28
3.13	Prestress Anchorage and Jacking System . . . . .	29
3.14	Load Cells and Anchorage System . . . . .	30

---

3.15	Acting Forces within Prestressed System . . . . .	31
4.1	Section View of the Beams Formwork . . . . .	36
4.2	Completed Formwork . . . . .	37
4.3	Completed Formwork . . . . .	37
4.4	Custom Jig . . . . .	39
4.5	Completed Reinforcing Cage . . . . .	40
4.6	Steel Reinforcing Chairs . . . . .	41
4.7	Completed Cast Concrete . . . . .	42
4.8	Coompression Testing Cylinder Moulds . . . . .	43
4.9	Compression Testing of the Concrete Cylinders in the Avery Machine . . . . .	44
4.10	Testing System including Prestressing and the System 5000 . . . . .	45
4.11	Labelling of the Flexural Steel Strain Gauge . . . . .	46
4.12	Application of Shear Reinforcement Strain Gauges . . . . .	47
4.13	Multimetre, Adhesive and Acetone . . . . .	48
4.14	Top Concrete Strain Gauges . . . . .	49
4.15	System 5000 Strain Gauge Data Lines . . . . .	49
4.16	LVDT . . . . .	50
4.17	Load Cells in Position for Initial Prestressing . . . . .	50
4.18	Hydraulic Jack and Prestressing Apparatus . . . . .	51

---

5.1	The Load versus Deflection for Control Beam 1 . . . . .	55
5.2	Mid-Span Flexural Cracking of the Control Beam . . . . .	56
5.3	Load versus Deflectionf for Control Beam 3 . . . . .	57
5.4	Local Crushing of the Concrete Mid-Span of the Beam . . . . .	58
5.5	Load Versus Deflection for Prestressed Beam 2 . . . . .	59
5.6	Load Versus Deflection for Prestressed Beam 4 . . . . .	60
5.7	The Load versus Deflection for the Control Beam and Prestressed Beam of Loading Position of $A = 1\text{m}$ . . . . .	63
5.8	The Load versus Deflectionf or the Control Beam and Prestressed Beam for Loading Position of $A = 0.5\text{m}$ . . . . .	64
5.9	The Load versus Deflection for the Control Beams . . . . .	65
5.10	The Load versus Deflection for the Prestressed Beams . . . . .	66
5.11	Propogation of the Shear Cracks Formed . . . . .	67
5.12	Typical Flexural Crackign Pattern for All Test Specimens . . . . .	68
5.13	Increase in Prestressing Force . . . . .	74

# List of Tables

3.1	Mechanical Properties of External Prestressing Bars, (Source-SAA HB64, 2002),Guide to Concrete Construction, pg 17.5, table 17.1 . . . . .	28
5.1	Strain Gauge Labels and Relevant System 5000 Input Lines . . . . .	53
5.2	Compression Test Results . . . . .	54
5.3	Percentage Increase in Flexural Strength after Prestress . . . . .	64
5.4	Percentage Decrease in Deflection after Prestress . . . . .	65
5.5	Theoretical versus Experimental Flexural Control Beam Results . . . . .	69
5.6	Theoretical versus Experimental Flexural Prestress Results . . . . .	69
5.7	Recorded Values of Prestressing Force within the Prestressing Tendons .	72
5.8	Recorded Value of Force versus the Predicted Force using the Recorded value of Force within the Tendons . . . . .	73

# Chapter 1

## Introduction

### 1.1 General Background

Concrete, in its most basic form, is a mixture of cement, water and fine and coarse aggregates (sand and crushed rock or natural gravel), which is plastic when first mixed, but which then sets and hardens into a solid mass. When plastic, it can be moulded or extruded into a variety of shapes. When hardened, it is strong and durable, able to support substantial loads and, at the same time, resist the effects of fire, weather, wear, and other deteriorating influences. It is, therefore a construction material of great versatility and wide application (SAA HB64, 2002).

The properties of concrete in both the plastic and the hardened states are dependant on the physical characteristics, the chemical composition, and the proportions of the components used in the mixture. Thus by varying the components, the type of concrete made can vary. Other forms of cement available are Blended cements; High-early strength cements, which as suggests gains high strength earlier than Portland cements; Low heat cements, used where limits are placed on the temperature rise associated with the heat of hydration; Shrinkage limited cements; Sulphate resisting cements along with various other commercially available cement mixes.

Reinforced concrete was invented by a Joseph Monier in 1861, and the concept of reinforcement concrete was patented in 1867. Reinforced concrete is a combination

of steel and concrete. Concrete's compressive strength is high, making it ideal for members loaded under compressive forces. Columns and arches are perfect examples of where concrete high compressive strength can be used. Concrete is a relatively brittle material, where its tensile strength is very low in comparison with its compressive strength, preventing its economical use in structural members subject to tensile forces or biaxial loading. "To offset this limitation, it was found possible, in the second half of the nineteenth century, to use steel with its high tensile strength to reinforce concrete" (Nilson, Darwin, Dolan, 2004). The inclusion of steel also enables designers to allow for a ductile failure, instead of what could result in brittle failure if the tensile forces were in fact carried by the concrete. In reinforced concrete the compressive forces are carried by the compressive area of the concrete, and the tensile forces are in part taken by the area of steel provided in the tensile section of the reinforced concrete. The concrete cover which exists over the steel acts as a durable fire and wear resistant barrier, protecting the steel. The aim of the reinforced concrete designer is to combine the reinforcement with the concrete in such a manner that sufficient of the relatively expensive reinforcement is incorporated to resist the tensile and shear forces which may occur, whilst utilising the comparatively inexpensive concrete to resist the compressive forces (SAA HB64, 2002).

This resulting combination of steel and concrete is a relatively low cost material with good weather and fire resistance, good compressive and tensile strength, high workability and formability. These above characteristics make reinforced concrete an excellent structural material, where present day construction purposes include buildings, bridges, dams, tanks, reservoirs and many other uses. The widespread structural and commercial use of construction using concrete stems from its availability and cheapness.

Prestressed concrete, like reinforced concrete is a composite material. The main purpose of using prestressing on a flexural member is to improve its load capacity behaviour, created by an induced force which in turn creates an internal moment which opposes that of the moment created by the imposed service loads. Resulting in less deflection and cracking of that flexural member.

Time dependent reduction in the prestressing force, due to creep and shrinkage of the concrete and relaxation of the prestressing steel tendon are but a few long term

losses associated with prestressing. These losses must be taken into account for the expected loading during the members service life for a successful implementation of the technology to be in fact successful. Other problems that arise from external prestressing are the long term durability problems associated with the external unbonded tendons. Long term maintenance and supervision are required.

At present, the application of external prestressing to deteriorating, overloaded or aging existing structures/members using unbonded tendons is proving to be a very effective and promising means of strengthening structural elements or systems. Even in well designed concrete members cracking is the main cause of failure. This can lead to loss of structural integrity allowing partial or total collapse mechanisms to occur. The applications of external prestressing type rehabilitation techniques have been shown to not only increase the life expectancy of the member or system, but to increase the flexural strength considerably, resulting in reduced deflection and crack widths. The application of such models is still considered a growing technology in Australia. This document will attempt to explain the background of the essential components within the external prestressing system. It will also discuss the results that this research has achieved, furthermore will hopefully add to the advancement of the research into this exciting technology.

## **1.2 Research Aim and Objectives**

This project aims to investigate the variation in flexural strength of rectangular reinforced concrete beams with the application of an external prestressing. Also to monitor the deflections and cracks formed under loading condition. Some major aims of the project are as follows:

- To develop a sound external prestressing application technique.
- To obtain the magnitude of the change in the specimens flexural strength after external prestressing.
- To observe and compare the change in the specimens deflections and crack widths.



- To compare the experimental results with the theoretical predictions.
- Discuss other unexpected outcomes of the experimental phase.

External prestressing offers a viable strengthening and rehabilitation tool for aging, overloaded or weakening members. This technology can therefore help to strengthen all existing flexural members in which the external prestressing can practically be applied to, including bridge girders and structural beams. The aim of this project is to compare the increase in flexural strength from the prestressed concrete beams with the non-prestressed concrete beams under two different loading conditions. These 2 loading conditions can somewhat represent or model the loading patterns that such flexural member will experience in service. With the inclusion of the external prestressing, not only will the flexural strength be increase, but the deflection decreases, and any cracks minimised. Hopefully the results of the project show that given an aging or weakening member of similar proportions and under similar loading conditions, the methodologies discussed could be used to extend the members service life, and or to increase its service capacity without the need to replace the member.

This thesis developed and analysed the flexural strengthening of reinforced concrete beams using the application of external prestressing. Such advancements are required for the strengthening and rehabilitation of new or existing concrete structure. The forever aging, weakening and overloading of our current concrete structures requires such methods.

### 1.3 External Prestress

External prestressing refers to a post tensioning method in which prestressing tendons are not enclosed or bonded within the concrete, rather are “external” and attached through a series of anchor points. Thus the prestress force is transferred via these anchor points as a compressive force into the beam itself. The prestressing principle is believed to have been well understood since about 1910, although patent applications related to types of construction involving the principle of prestressing date back to 1888 (Libby, 1984).

Pre-tensioning and post-tensioning are forms of prestress. Where post-tensioning of the tendon occurs after the concrete has sufficient strength to support the prestressing force. This method is usually used primarily for in-situ construction. In pre-tensioning the tendon is prestressed before the concrete is cast. Usually formed in a Workshop environment and transported to site. In the case of external pre-tensioning, the order in which the stress is applied does not vary but rather whether the tendon is contained within the beam itself and or bonded or unbonded. In prestressed concrete members, the concrete is placed in compression, the compression force is formed from the force or stretching of the tendons (strands or bars) either bonded or non-bonded, transferring the compression force to the concrete via the anchor points. This compressive force acts to then place the concrete in compression which enables the member or system to withstand a greater service flexural loading. The moment induced from the prestressing force, along with the eccentricity of the tendon act against the load induced moment from imposed and permanent loads, thus prestress increases the load capacity of the member.

As the tendons themselves, or in the case of this project, the high tensile bars are external to the safety of the durable concrete, the bars are therefore exposed to the elements and deterioration of the bars can occur without proper precautions. Surveillance and maintenance measures are necessary, including the maintenance of the prestressing force within the tendons, as this can decrease with time, and a re-stress may be necessary.

Some of the advantages and limitations of this style of external prestressing on in service flexural members have been produced below:

Advantages of Externally prestressed Unbonded Tendons:

- The tendon placement and adjustment is carried out separately to the concrete placement and concrete works.
- Implementing external prestress on existing works as it stands, without undue moving or dismantling the structure.
- If effectively initiated, the cracking due to overloading or aging will be closed

completely without the need for crack strengthening techniques, rather crack durability control techniques.

- The tendons are easily accessed for re-stressing and can be easily maintained or replaced.
- The prestressing bars can be easily mounted and transported, as the bars are a rigid stiff medium given the side area of the flexural member is available.
- Given that this project uses high tensile threaded bars as the prestressing tendon, the prestressing force is easily maintained and varied with plates and nuts threaded onto the rod.

Limitations of Externally prestressed Unbonded Tendons:

- The room required for the placement and stressing of the tendon may not always be considered in the design of the specimen and can limit such prestressing applications.
- The tendons used in external prestressing techniques are exposed to the elements (fire, chemicals, weather, etc.), and can deteriorate without proper supervision and maintenance. Costs over time are then implicated from such maintenance measures.
- External bars extruding from the structure along the flexural members can be very unsightly and detract from the aesthetics of a structure.

## 1.4 Dissertation Overview

An overview of the dissertation will now be included to prompt the reader of its contents and the structural format of the this project.

### Chapter 2

This chapter gives a detailed review of external prestressing, including historical background of the prestressing technique and how the technique have developed. This chapter also attempts to explain the theory or purpose behind this study. Various theoretical studies will be sourced.

**Chapter 3**

This chapter gives an overview on the specimen design. This will include all flexural and shear calculations, including moment and shear diagrams. Shear reinforcing and spacing is also be covered. Finally the design of the external prestress that was used will be discussed.

**Chapter 4**

This chapter will discuss the experimental methodology used in this study, the procedure undertaken throughout the testing of the specimens, including the various processes and preparation techniques undertaken will be discussed.

**Chapter 5**

This chapter will discuss all results obtained throughout the testing phase. Comparisons between tests, and also comparisons between the theoretical predictions and experimental results will be shown.

**Chapter 6**

In this chapter the final conclusion on the projects testing and results will be made. This chapter also strives to conclude on the aims of the research set out to be achieved and gives recommendations for further study.

**1.5 Summary**

This thesis aims to inform the reader how the project results and conclusions were developed and achieved. All experimental data will be compared with the theoretical data, and conclusions on any observations will be made. The research made will hopefully result in further applications into this style of prestressing, and also the understanding of how flexural members behave under loading conditions similar to those tested. The outcomes of this study will hopefully provide enough data for finite element techniques and further research into the areas of the test specimens stressed and why the concrete cracked where it did.

## Chapter 2

# Review of External Prestressing

### 2.1 Introduction

Prestressing is the creation within a material of a state of stress and deformation that will enable it to better perform its intended function, as the stresses induced by the prestressing oppose that of the imposed stresses from loading. Prestressing can be and has been applied to many materials including concrete, steel, stone, ceramics, brick, timber, native rock and soil. The prestressing principle is believed to have been well understood since about 1910, although patent applications related to types of construction involving the principle of prestress date back to 1888. The early attempts at prestressing were abortive, however, owing to the poor quality of materials available in the early days as well as to a lack of understanding of the action of creep in concrete. Prestressed concrete has gone through research and development phases during the 1930's and 1940's, and through specialised design and specialised construction phases from 1955 to the present. Because of the minimal additional weight of the repair system, this technique is effective and economical, and has been employed with great success to correct excessive deflections and cracking in beams and slabs, parking structures and cantilevered members.

As stated in SAA HB64 (2002) "Prestressed concrete may be defined as reinforced concrete in which the reinforcement, high tensile steel wires or bars, is stretched or

tensioned before being bonded with the concrete in some way. The force in the steel is transferred to the concrete, placing it in compression and thereby increasing its ability to withstand tensile forces. The development of prestressed concrete has enabled greater spans and more slender structures to be achieved”.

## 2.2 Historical Development

The first worldwide externally prestressed concrete bridge built, was in Aue, Saxony between 1935 and 1937. The bridge was based on a proposed concept by Dischinger (DRP 727 429). The beam bridge had variable depths, with three spans (25.2 m - 69.0 m - 23.4 m). Suspended unbonded tendons running outside the concrete cross-section were used. However corrosion of the unbonded tendons and a high loss of prestress caused by creep and shrinkage within the concrete led to major problems with the bridges function.

Proceeding 1945, developments in bridge construction within Germany were concentrated on internal post-tensioned systems. However, in both Belgium and France external prestressing was being implemented. In Germany the corrosion resistances of external tendons were considered to be inadequate at that time, whereas post-tensioned bridges with internal tendons appeared unproblematic and so only this construction method was further developed and applied (VSL Report Series, 1999).

Wayass and Freytag designed and constructed a bridge over the Dortmund-Hannover Autobahn in Oelde, FRG, in 1938, where for the first time high tensile prestressing steel arranged inside the concrete section was used for 4 simply supported girders of 33m spans. This bridge used methods which are commonly referred in the present as conventional prestressed concrete. Also in the year of 1938, Finsterwalder developed his concept of the “self-stressing concrete beam”, which was put to actual test for the bridge over the same Autobahn at Rheda-Wiendenbruck, FRG (a simply supported girder of 34.50m span). The bar tendons were later encased in concrete, giving rise to the “self-stressing” system. During the years of 1938 to 1943, Haggbohm designed and built the Klockestrand Bridge near Stockholm, Sweden. For the main spans the

Dischinger concept was applied. The main span superstructure was prestressed with a total of 48 bars of 30 mm with a yield strength of 520 N/mm. The constructed bridges are still in service today after 50 years of use (VSL Report Series, 1999).

During the late 1950s, the first applications of external prestress for the strengthening of existing structures can be found. An early example is the two span steel truss bridge, spanning 48 - 48 m over the River Aare at Aarwangen, Switzerland. The bridge was originally built in 1889 and was no longer capable of supporting increasing modern traffic loads. In 1967 the bridge was strengthened using external prestressing techniques. A rebirth of the external post-tensioning techniques can be observed from the mid-seventies onward (VSL Report Series, 1999).

In 1978-1979 Muller introduced external post-tensioning in the United States, for the Key Bridges in Florida. His main goals were speed of construction and economy. Since 1980, many bridges have been designed and built using either external tendons or a combination of internal and external tendons.

## **2.3 Previous Studies**

External prestressing has become an integral part of the strengthening and rehabilitation of aging, weakening and over loading of Australia's reinforced concrete members and structures. Abstracts of AS 3600 in HB 2.2 - 2003, the concrete structures design code for Australia, has been used for all matters entailing to the design of the concrete members. This maintains that the specimen design will be to an Australian recognised minimum standard. "This standard sets out the minimum requirements for the design and construction of concrete structures and members that contain reinforcing steel, or tendons, or both" (HB 2.2 -2003). These standards are in place to ensure that the construction industry of Australia remains a "structurally" safe environment. This can also include the factors involved with serviceability and durability where the member itself may be strong enough, but will sag or crack and with time corrode and leave unsightly stains. "The aim of structural design is to provide a structure that is durable, serviceable and has adequate strength while serving its intended function and

that satisfies other relevant requirements such as robustness , ease of construction and economy” (HB 2.2 -2003). Thus all factors encountered in a members life are again taken into in my specimen design, account according to AS 3600. Other texts exist for the calculation of the moment and shear capacities, using variations and simplifications or formulas, but I have chosen to simply stick with the Australian standard AS 3600. This then gives a well known and highly regarded text to which the public can relate and reference the theories I have chosen to use.

Sayed-Ahmed, Riad and Shrive (2004) showed that experimental work carried out in Canada, using the externally post-tensioned bars on reinforced concrete bridge girders yielded a 19% flexural strength increase. The document discusses how the experimental flexural strength after post tensioning was 2% below the expected theoretical increase. These results were very encouraging, and the document states that this “classical” type approach of external post-tensioning should not be disregarded, confirming the existence of further studies, like my research into the field of external prestress using the “classical” style approach. The document refers to the external post tension using steel bars as the ”classic” approach, in relativity to the new materials such as fibre composites that are currently being experimented with in similar rehabilitation and strength increasing programs.



## Chapter 3

# Specimen Design

### 3.1 Introduction

This chapter will describe the different approaches that were considered for the construction of the flexural test specimens used for the testing phase of this project. The chapter will describe the analytical calculations undertaken in the specimen sizing or beam dimensions and demonstrate the reinforcing steel required to achieve the required flexural and shearing strengths of the design section given the loading conditions. The external prestressing capacity calculation of the section will also be shown.

### 3.2 Specimen Design Approach

The test specimen chosen for the flexural testing throughout this study were rectangular concrete reinforced sections. The rectangular section is not the most material efficient section in flexural bending in comparison with a T-shaped member, though a rectangular section suited what resources were made available and will act similarly under induced flexural loads. For flexural members the “T” section is usually used as the thin webs allow for the external prestressing to be placed without the prestressing apparatus protruding from the side of the beam. Though for the purpose of the flexural strength testing phase of this study, a rectangular reinforced and prestressed section

was deemed satisfactory.

The test specimens failure in flexure was a design parameter required to be achieved, therefore the force required to fail the beam in flexure was much less than the force required to fail the beam in shear. Thus the shear capacity of the beam is larger than the flexural capacity of the beam. The beams were designed as simply supported beams. Also with the application of the external prestress and prestressing force, the flexural capacity of the beam will increase, and thus the force required to fail the beam will also.

Two loading points have been chosen to demonstrate the flexural capacity of the design beams. A total of four test beams were chosen, where two control beams and two prestressed beams were proposed. Thus a control and prestressed beam existed for each loading position. Shown below are the bending moment diagram and shear force diagram for the test beams under the designed point loading positions.

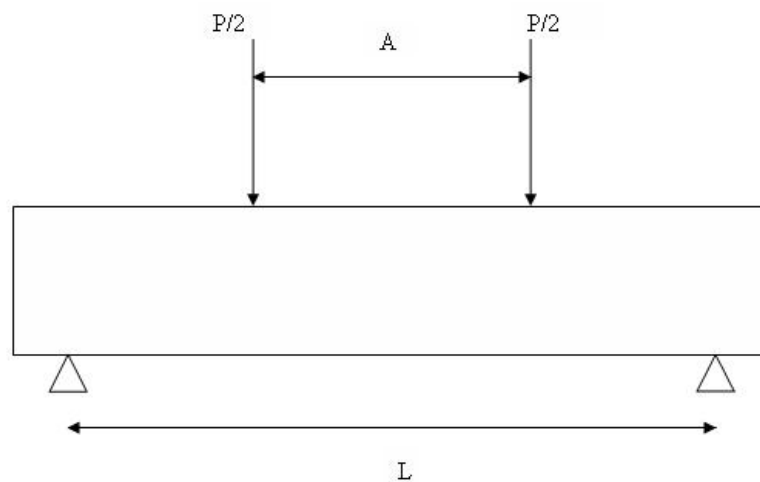


Figure 3.1: Loading Position Arrangement for Test Beams

Loading Position of the Test specimens  $A = 1$  m

$A = 0.5$  m

As it can be deduced from Figure /reffig:Figure32, the maximum bending moment which exists within the test specimens under the given loading positions exist mid-span of the 3500 mm spanning beam.

Bending Moment Diagram at loading position,  $A = 1$  m

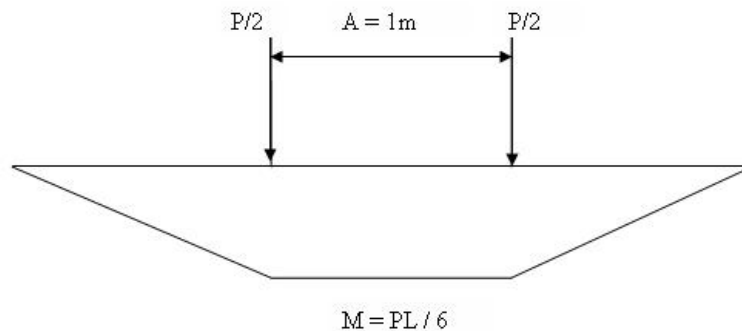


Figure 3.2: Bending Moment Diagram at  $A = 1$  m

Bending Moment at Loading position,  $A = 0.5$  m

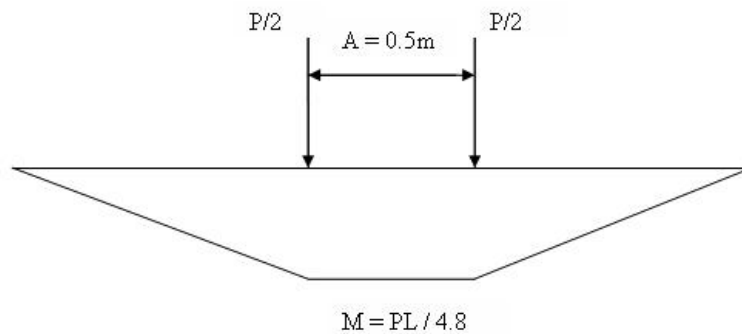


Figure 3.3: Bending Moment Diagram at  $A = 0.5$  m

It can be seen from the bending moment diagram in Figure 3.2 and Figure 3.3 that the maximum bending moment occurs at mid-span of the beam. As the flexural strength is critical, it can be therefore seen that the mid section of the beam is the critical section. This therefore is the section of the beam which is under the maximum moment and thus the most consideration. It can be observed from the shear force diagram (Figure 3.4) that the mid-span is not the section that is critical in shear, but rather the region from the beams supports to the loading points, where the shear force,  $V = P/2$ .

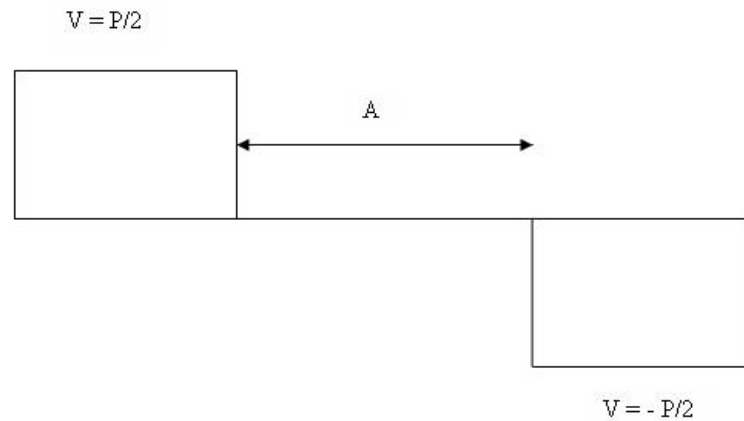


Figure 3.4: Shear Force Diagram

This identified shear region therefore requires considerable observation when undertaking the physical testing of the specimen, as to observe any shear cracks that may form, when loaded in both loading positions. Shear failure is not an expected outcome, as consideration has been taken in the design for the beam not to fail in shear.

The specimen design initiated with assumed dimensions, relevant to the resources available, including the materials and testing facilities. The beams were to be post-tensioned beams with external unbonded high tensile threaded bars anchored at either end, with the beam simply supported at 3000 mm. Once an initial estimate of the specimen design was achieved, initial design calculations were undertaken to check all the design criteria.

### 3.3 Beam Specimen Design

This section will describe the more detailed design of the beam section itself, where the beam dimensions; reinforcing and prestress placement are shown.

### 3.3.1 Beam Dimensions

The 4 test beams were all rectangular reinforced sections, with external un-bonded post-tensioned high tensile threaded bars. The simply supported beams span 3500 mm, with section dimension of 300 x 150 mm.

Figure 3.5 and Figure 3.6 are typical of all 4 beams and give the front and side view of the specimens:



Figure 3.5: Front View of Design Specimen

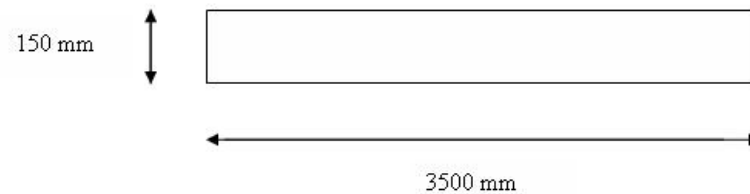


Figure 3.6: Top View of Beam Specimen

Typical cross-section of the 4 beams specimens is shown below in figure 3.6 :

It can be seen in Figure 3.7, that the depth of the section is 300 mm and the width of the section is 150 mm, making the 300 x 150 mm typical cross-section. Also shown in Figure 3.7 is the cover that was used in the concrete beams. The concrete cover was found in accordance with AS 3600 to be 25 mm. A major design parameter or limitation was that the test beams section dimensions had to be manageable with the University Laboratory when preparing and testing the beams.

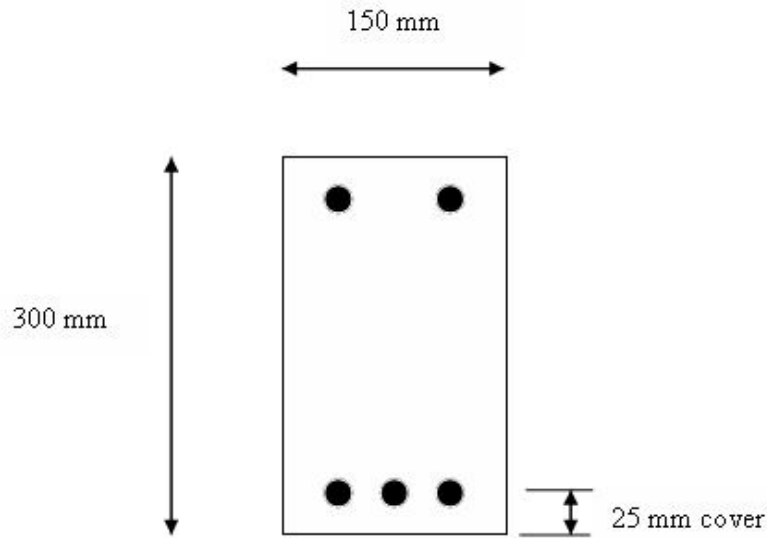


Figure 3.7: Typical Cross-Section of Beam Specimen

### 3.3.2 Steel Reinforcement

Steel reinforcement was used in the compression and tensile areas of the beam, including shear reinforcement. All steel chosen to reinforce the tensile and compressive zones was chosen to achieve the required shear and flexural strength set by the limitation of the shear strength exceeding that of the flexural strength. Shear reinforcement was therefore on the conservative side.

As seen in figure 3.4 the shear regions exist from the loading point to the supports of the simply supported beams. The general spacing of the shear reinforcing was 200 mm, throughout the middle 2400 mm of the test specimens. Though to enable that the shear reinforcement was sufficient in the regions depicted in the shear force diagram, the shear ligature spacing was reduced to 100 mm within the last 400 mm of the beam, as shown in Figure 3.8. The reduced spacing also reinforcing the concrete areas where the prestressing bars anchoring plates reside, or where the compressive force from the prestress is induced into the concrete. The close spacing of the stirrups at the ends of the beams also helps the beam resist the axial force (induced to the beam in the

longitudinal direction). The shear ligatures were hand bent N-6 bars. The remainder of the beam was designed using 200 mm spacing.

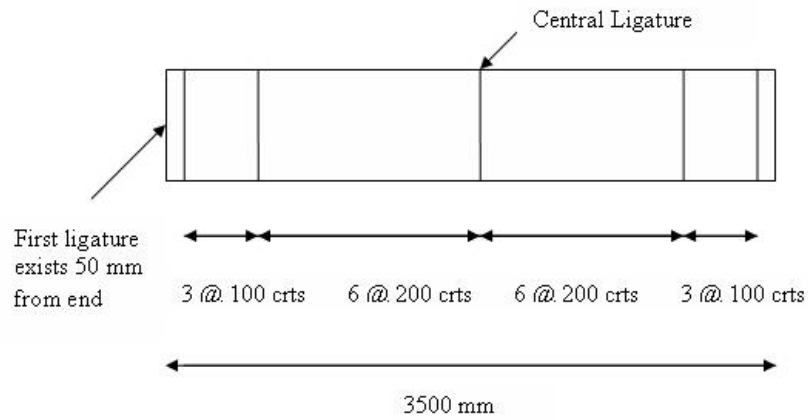


Figure 3.8: Shear Reinforcing Spacing

2 N-12 bars were chosen to be used in the top compression reinforcement, and 3 N- 12 bars were chosen to be used in the bottom tensile reinforcement.

The typical steel reinforcing layout can be shown below in Figure 3.9, which was typical for all 4 beams, both prestressed beams and the control beams.

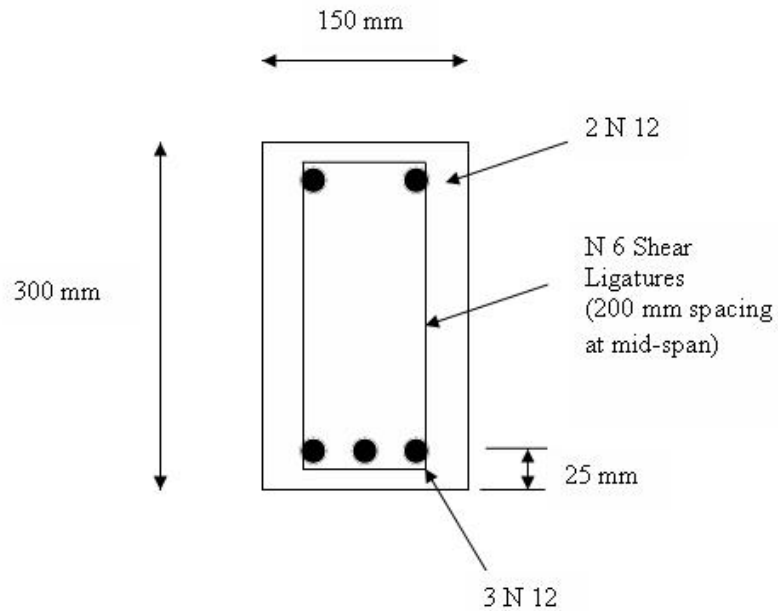


Figure 3.9: Typical Section Reinforcing

At each end where the ferules were placed for the attachment of the anchorage plate, short lengths of N-6 bars were also used.

No extra reinforcing was used in the reinforcing of the ends of the beams where the force is applied; it was assumed that the close spacing of the ligatures in the last 400 mm of the beam would be sufficient.

### 3.4 Control Condition Strength Capacity

This section deals with the computations of the moment and shear capacity of the test beams. All computations were carried out in accordance with AS 3600, the Australian Standard for Concrete Structures. The calculations were carried out for the mid-span section of the beam, as this is the critical area.

Calculation of the Moment Capacity of the control beams.

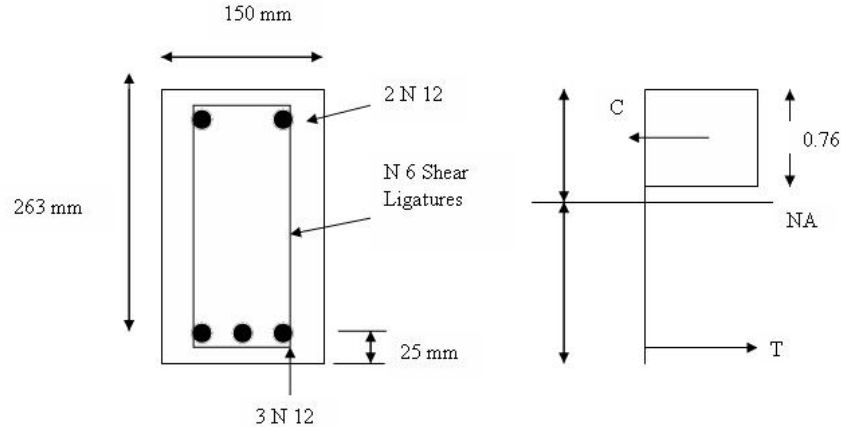


Figure 3.10: Mid-Span Section Flexural Analysis

Tensile Steel Area,

$$A_{st} = (3 \times 12mm \text{ diameter bars}) = 3 \times 110 = 330 mm^2$$

Compressive Steel Area,

$$A_{sc} = (2 \times 12mm \text{ diameter bars}) = 2 \times 110 = 220 mm^2$$



$E = 200\,000\text{ MPa}$

For N 12 bars,

$$f_{sy} = 500\text{MPa}$$

For N 6 bars,

$$f_{sy} = 250\text{MPa}$$

Concrete Compressive Strength,

$$f_c = 40\text{MPa}$$

$b = 150\text{ mm}$  (beam width),

Cover = 25 mm, in accordance with AS 3600,

For the Ultimate Moment Capacity, clause 8.1.2.2, AS 3600.

Effective Depth,

$$\begin{aligned} d &= 300 - 25 - 6 - (12 \div 2) \\ &= 263\text{mm} \end{aligned}$$

Therefore to find  $\gamma$ ,

$$\begin{aligned} \gamma &= 0.85 - 0.007 \times (f_c - 28) \\ &= 0.85 - 0.007 \times (40 - 28) \\ &= 0.766 \end{aligned}$$

Neutral Axis depth,

$$d_n = k_u \times d \tag{3.1}$$

Where  $k_u$  is the neutral axis parameter,

$d$  is the effective depth of the section.

Therefore, the sections design compressive force shown in equation 3.2,

$$C = 0.85 \times f_c \times \gamma \times b \times d_n \tag{3.2}$$

$$\tag{3.3}$$

$$= 0.85 \times 40 \times 0.766 \times 150 \times k_u \times 263, \text{ where } (d_n = k_u \times d)$$

Therefore, the sections design tensile force can be shown in equation 3.4,

$$\begin{aligned} T &= A_{st} \times f_{sy} \\ &= 330 \times 500 \end{aligned} \quad (3.4)$$

To achieve equilibrium of the internal forces within the section,

$$\begin{aligned} \text{Compressive Force (Equation 3.2)} &= \text{Tensile Force (Equation 3.4)} \\ 0.85 \times 40 \times 0.766 \times 150 \times k_u \times 263 &= 330 \times 500 \end{aligned}$$

Rearrange equation 3.1 for the calculation of the neutral axis parameter  $k_u$

$$k_u = 0.16$$

Therefore the neutral axis depth,

$$\begin{aligned} d_n &= 0.16 \times 263 \\ d_n &= 42.2 \text{ mm} \end{aligned}$$

Strain diagram of the internal strains within the section

From the above strain diagram, Figure 3.11 it can be seen through similar triangles the strain in the tensile steel reinforcing,

Therefore to calculate the strain in the tensile steel  $\varepsilon_s$

$$\begin{aligned} \varepsilon_c/42.2 &= \varepsilon_s/220.8 \\ \varepsilon_s &= (0.003/42.2) \times 220.8 \\ \varepsilon_s &= 0.0156 \end{aligned}$$

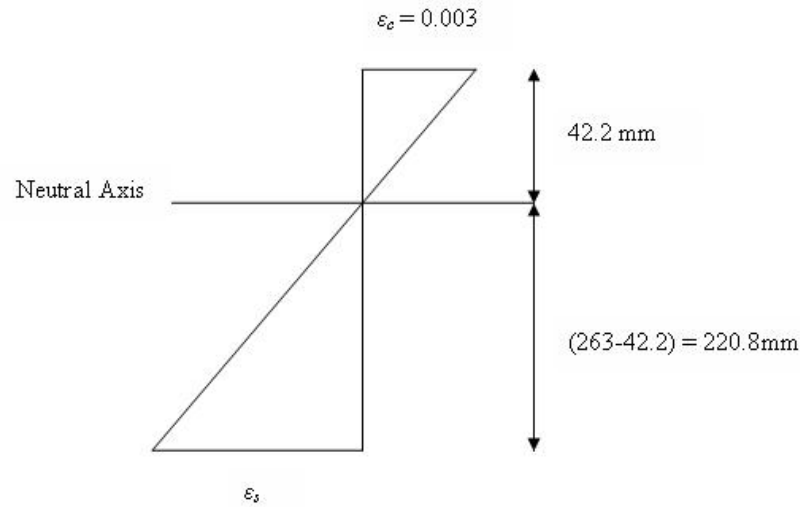


Figure 3.11: Strain Diagram

Therefore as,

$$\epsilon_s = 0.0156 > 0.002,$$

Therefore it can be seen that the tensile steel has yielded as  $\epsilon_s > 0.002$ . It can also be noted that the tensile steel has yielded from the balanced section formula techniques when  $k_u < 0.4$ . Therefore the under reinforced section of the control beams will undergo a ductile failure.

Therefore to calculate the ultimate moment capacity for the non-prestressed section or the control beams condition (Equation 3.5):

$$\begin{aligned} M_u &= f_{sy} \times A_{st} \times d \times (1 - 0.5 \times \gamma \times K_u) \\ &= 500 \times 330 \times 263 \times (1 - 0.5 \times 0.766 \times 0.16) \\ &= 40.7 \text{ kN.m} \end{aligned} \quad (3.5)$$

Therefore it can be seen that the ultimate bending capacity of the control beam sections is 40.7 kN.m.

Also to calculate the force required to induce the above moment and in-fact fail the control beams in bending is calculated and shown below:

Finally it can be seen in Figures 3.2 (b) and Figure 3.2 (c), for the 1 m and 0.5 m loading positions respectively:

Effective Spanning Length = 3 m.

Therefore for the 1 m loading position,

$$M = (P \times L) \div 6$$

Thus,

$$\begin{aligned} P &= (6 \times M) \div L \\ &= (6 \times 40.7) \div 3 \\ &= 81.4kN \end{aligned}$$

And for the 0.5 m loading position,

$$M = (P \times L) \div 4.8$$

Thus,

$$\begin{aligned} P &= (4.8 \times M) \div L \\ &= (4.8 \times 40.7) \div 3 \\ &= 65.1kN \end{aligned}$$

Therefore the maximum load that the section can take before prestress (control condition) is 81.4 kN for the loading position of  $A = 1\text{m}$ , and then 65.1 kN for the loading position of  $A = 0.5\text{ m}$ . These are the theoretical values that have been calculated for the force required to fail the test beams in flexure.

Calculation of the Shear Capacity of the control beams.

The calculation of the shear capacity of the control beam section follows briefly:

Tensile steel area,

$$A_{st} = (3 \times 12mmbars) = 3 \times 110 = 330mm^2$$

Compressive steel area,

$$A_{sc} = (2 \times 12mmbars) = 2 \times 110 = 220mm^2$$

Shear ligatures reinforcing steel,

$$A_{sv} = (2 \times 6mmbars) = 2 \times 28 = 56.5mm^2$$

For N 12 bars,

$$f_{sy} = 500MPa$$

For N 6 bars,

$$f_{sy} = 250MPa$$

Therefore the compression strength of the concrete,

$$f_c = 40MPa$$

b = 150 mm (beam width),

Cover = 25 mm, in accordance with AS 3600,

For the Ultimate Shear Capacity, clause 8.2.7.1 and clause 8.2.10 from AS 3600.

Assumed that,

$$\beta_3 = \beta_3 = 1$$

Shear ligature spacing of 200 mm were used. The spacing of the steel ligatures is as low as 100 mm near the ends of the beams, but for the sake of the general shear strength

of the shearing area from beam supports to the point loading positions, the worst case of 200 mm spacing will be used.

The shear capacity formula used from AS3600 is of the form shown below (Equation 3.6), where the shear capacity is made up of the shear capacity of the concrete and the shear capacity for the shear reinforcement.

$$V_u = V_{us} + V_{uc} \quad (3.6)$$

Therefore, the shear capacity of the concrete is given in equation 3.7 below:

$$V_{uc} = \beta_1 \times \beta_2 \times \beta_3 \times b_v \times d_o ((A_{st} \times f'_c) \div (b_v \times d_o))^{1.3} \quad (3.7)$$

This function shows the calculation of the factor  $\beta_1$ ,

$$\beta_1 = 1.1 \times (1.6 - d_o) \div 1000 = 1.1 \times (1.6 - 263) \div 1000 = 1.47$$

Hence substituting Equation 3.8 into equation 3.7,

$$\begin{aligned} V_{uc} &= \beta_1 \times \beta_2 \times \beta_3 \times b_v \times d_o ((A_{st} \times f'_c) \div (b_v \times d_o))^{1.3} \\ &= 1.47 \times 1 \times 1 \times 150 \times 263 \times ((220 \times 40) \div (150 \times 263))^{1.3} \\ &= 40.3kN \end{aligned}$$

Shown below is Equation 3.8 that AS3600 has adopted for the accessing of the shear capacity of the steel shear reinforcement:

$$\begin{aligned} V_{us} &= ((A_{sv} \times f_{sy} \times d_o) \div s) \times \cot\phi_v \quad (3.8) \\ &= ((56.5 \times 250 \times 263) \div 200) \times \cot\phi_v (\text{where } \phi_v = 45) \\ &= 22.7kN \end{aligned}$$

Therefore by inputting the results from Equations 3.7 and 3.8 into equation 3.6, the shear strength of the reinforced section can be calculated

$$\begin{aligned}V_u &= V_{us} + V_{uc} \\ &= 22.7 + 40.3 \\ &= 63kN\end{aligned}$$

The strength prediction equations of AS 3600 predict that given the section of concrete and the steel reinforcement of the design section, the beam will fail in shear with a total shearing force of 63 kN.

Hence, the force required to therefore fail the beam in shear, given the two loading points.

As can be seen in Figure ??, the shear force is  $V = P / 2$ , thus as the shear force  $V$  is known, the force  $P$  can be found.

$$V = P/2$$

Hence,

$$\begin{aligned}P &= 2 \times V \\ &= 2 \times 63 \\ &= 126kN\end{aligned}$$

Thus the force required to fail the beam in shear is 126 kN. As stated this force is greater than the 60 -82 kN force to fail the beam in flexure.

### 3.5 Prestress Design

The prestress design that was chosen for this test was the typical style post-tensioning external bars. These bars exist with no eccentricity and the eccentricity that does occur due to second order effects for this project was neglected. The Prestress tendon chosen for this design was a 23 mm (nominal diameter) high tensile threaded steel bar.

Two bars for each prestressed beam were used, where these bars were at set positions and the eccentricity of the 2nd order effects caused as the beam deflects were assumed negligible. The prestressing area of the two bars was 415 mm<sup>2</sup> and carried a designed prestress of 80 kN each, for a total prestressing force of 160 kN. The bars were set to the ends of the concrete beams via two steel anchoring plates that for the sake of the tests were sufficient. Through attaching these plates with cast in ferrules, the prestressing bars were held 100 mm from the base of the beam. This enabled that the bars existed in the middle 2/3 of the beam. Also, these plates were available and were used with other students, making them more attractive for the tests. These methods listed below assume that the steel has yielded and will result in the stresses within the external tendons under the prestressing action. The equation used for predicting the flexural strength of the prestressed beams was an equation used on un-cracked sections. Though the beams in this project will in-fact be initially cracked, to achieve the “in-service” state of a overloaded or aged flexural member. The equation is still applied throughout the project as after the prestress has been applied, it is assumed that the prestressing forces magnitude is great enough to close all cracks and therefore the section will again act as a “new section”. These assumptions will be confirmed later in the research, where the percentage of flexural increase will occur only if this has been achieved.

The general form of the ultimate stresses in unbonded tendons can be expressed as follows:

$$f_{ps} = f_{pe} + \Delta f_{ps}$$

Where  $f_{ps}$  is the ultimate stress in the prestress tendons,  $f_{pe}$  is the effective initial prestress in the tendons and  $\Delta f_{ps}$  is the increment of stress in the prestress tendon.

For a member with a span to depth ratio of up to 35, AS 3600 clause 8.1.6 uses the following equation to calculate the stress in the unbonded tendon:

$$\varepsilon_{pu} = \varepsilon_{p.ef} + 70 + (f'_c \times b_{ef} \times d_p) \div (100 \times A_{pt}) \quad (3.9)$$

Where  $\varepsilon_{pu}$  is the ultimate stress in the prestressing tendon,  $\varepsilon_{p.ef}$  is the initial effective stress,  $A_{pt}$  is the area of prestressing steel which is in tension, which in the case of this project is generally equal to  $A_p$ .



Table 3.1: Mechanical Properties of External Prestressing Bars, (Source-SAA HB64, 2002), Guide to Concrete Construction, pg 17.5, table 17.1

Material Type	Nominal Diameter (mm)	Area ( $mm^2$ )	Minimum Breaking Load (kN)	Minimum Tensile Strength (MPa)
Bars - AS 1313	23	415	450	1080

Thus this formula will be used in accordance with the AS 3600 to calculate the theoretical values of the ultimate prestress stresses in the tendons. More of a discussion on the prediction equations capabilities will be discussed in chapter 5.

The properties of the prestressing bar are shown below; these attributes have been used in assessing the sections flexural strength after prestress has been applied:

The mechanical properties of the bars conform to AS 1313.

Shown below is the general layout of the prestressing design used in the externally post-tensioned tendons. The diagram demonstrates the use of the anchoring plates to transfer the compressive force and also the attachment detail of the cast in ferrules to hold the plate in place.

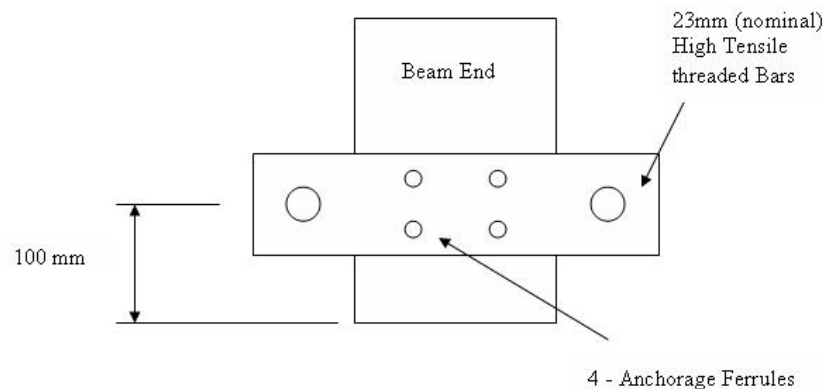


Figure 3.12: Cross Section of the Anchorage Plates and Prestressing Bars

Figure 3.13 shows the jacking system and external 23 mm high tensile threaded steel bars connected to the steel anchorage plate.



Figure 3.13: Prestress Anchorage and Jacking System

Figure 3.14 demonstrates the opposing end of the picture above. This end houses a similar anchorage plate, but also in place are some load cells which return to the system 5000 the measured prestressing load in the two external bars.

### 3.6 Prestressed Strength Capacity

The calculation of the maximum flexural capacity for the prestressed sections shown above in figure, are shown below.

Prestressing steel area,

$$A_{pt} = (2 \times 23mmbars) = 415mm^2$$

Therefore for the prestressing bars,

$$f_{py} = 1080MPa$$

Concretes compressive strength,

$$f_c = 40MPa$$



Figure 3.14: Load Cells and Anchorage System

$$E_p = 200000 \text{ MPa}$$

$$b_{ef} = 150 \text{ mm (width)}$$

$$d_p = 200 \text{ mm}$$

Tensile steel area,

$$A_{st} = (3 \times 12 \text{ mm bars}) = 3 \times 110 = 330 \text{ mm}^2$$

Compressive steel area,

$$A_{sc} = (2 \times 12 \text{ mm bars}) = 2 \times 110 = 220 \text{ mm}^2$$

For N 12 bars,

$$f_{sy} = 500 \text{ MPa}$$

For N 6 bars,

$$f_{sy} = 250 \text{ MPa}$$

Therefore using equation 3.9 shown below from AS3600, the ultimate stress in bending for the prestressing bars can be calculated:

Hence, with the newly calculated stress within the external tendon from equation 3.9, the relative forces within the tendons ( $T_p$ ) can be calculated. This involves a simple calculation where the force within the tendons is equal to the stress in the tendons multiplied by the cross-sectional area of the tendons. The force in the compression reinforcement and the force in the tensile reinforcement have both been assumed to have yielded and are calculated as shown below in equations 3.10 and 3.11.

The tensile and compression reinforcement have been assumed to have yielded and are calculated as shown:

$$F_{st} = A_{st} \times f_{sy} \quad (3.10)$$

$$F_{sc} = A_{sc} \times f_{sy} \quad (3.11)$$

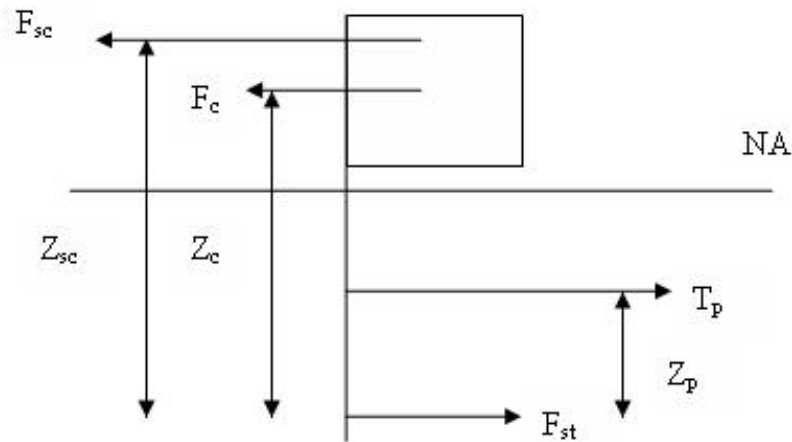


Figure 3.15: Acting Forces within Prestressed System

It can be seen from Figure 3.6 (a) that the forces in the section are at equilibrium, where the forces in the compression reinforcement and concrete are equivalent to the forces in the prestressing bars and the tensile reinforcement:

$$F_c + F_{sc} = T_p + F_{st} \quad (3.12)$$

Therefore by rearranging equation 3.12, the force in the concrete can be found:

$$F_c = T_p + F_{st} - F_{sc}$$

Hence, with the force in the concrete calculated the relative neutral axis depth can be calculated for the section after prestress using equation 3.13.

$$x = F_c \div (0.85 \times f'_c \times b \times \gamma) \quad (3.13)$$

Given the neutral axis depth on the section from equation 3.13, all the relevant lever arms can be calculated for the forces acting on the section, shown in Figure 3.6 (a).

With all the above information from equation 3.12 and 3.13, it is possible to calculate the new moment capacity for the section after the application of the prestressing force equation 3.14:

$$M_u = T_p \times Z_p + T_{st} \times Z_{st} + F_c \times Z_c + F_{sc} \times Z_{sc} \quad (3.14)$$

Then with the ultimate moment capacity ( $M_u$ ), found in equation 3.14, the force then required to fail the prestressed beam in flexure can be calculated. The force required to induce the calculated moment is found in the same fashion as discussed in the earlier force calculations for the control beams moments in section 3.4 of chapter 3.

The theoretical predicted ultimate strength values can be shown below for both the prestressed sections. The strengths for  $A = 1\text{m}$  and  $A = 0.5\text{ m}$  are shown after the application for the 160 kN prestress.

$A = 1\text{m}$ , Force required to fail the beam in flexure = 134 kN

$A = 0.5\text{ m}$ , Force required to fail the beam in flexure = 107 kN

## Chapter 4

# Experimental Methodology

### 4.1 Introduction

The experimentation of the concrete was carried out to model simply supported concrete flexural members that exist in service. The implementation of this testing was carried out with the loading positions and specimens that have been discussed prior to this chapter. The experimental methodology and preparation adopted for the flexural testing of the concrete beam specimens is described in this chapter.

This chapter will describe the preparation and groundwork that was carried out in the project. The chapter will describe the creation of the reinforcing cages, the formwork used, the pouring of the concrete and will continue to discuss all the instruments used in the testing phase of the experiments. Also the experimentation procedure, and beam setup will be discussed.

The experimental phase of this project required the use of large equipment, loads and deflections, which demands safety restrictions. Extra care and precautions were taken in the prestressing and de-stressing of the external tendons.

## 4.2 Experimental Procedure and Variables

As two loading position of  $A = 1\text{m}$  and  $A = 0.5\text{m}$  were being analysed for the test specimens a total of four beams were required. The beams had a rectangular cross section that remained consistent throughout all specimens. The prestressing depth remained constant over both tests. No eccentricity of the prestressing bars was analysed (No second order effects). The tests were carried out with the aim of achieving comparative result, where the specimens ultimate flexural capacity could be compared under the same prestressing condition, with variable loading positions. The positions were chosen to induce variation in cracking and deflection. Given the results of the tests a conclusion on the necessity of crack repair methods can be achieved, along with the effectiveness of this style of prestressing on flexural member under similar loading conditions. These results should give us a good indication of how the beam will act under a variety of loading conditions given a certain prestressing force.

The four beam specimens were a total length of 3500 mm with an effective span of 3000 mm. The beam sections were 300 x 150 mm rectangular sections. Loading positions of  $A = 1\text{m}$  and  $A = 0.5\text{ m}$  were the chosen spans between the two loading points. For the first test of  $A = 1\text{m}$  a I beam section cross beam was used, and for the second test of 0.5 m, a rectangular cross beam was used.

For the 1st and 2nd beams the loading position of 1m will be used. Beam 1 is the control beam and Beam 2 is the prestressing beam for the position of  $A = 1\text{m}$ . Therefore leaving Beam 3 to be the control beam and Beam 4 to be the prestressed beam for  $A = 0.5\text{m}$ .

Beam 1 was loaded initially without prestress. As the test was being carried out all information was being sent to the System 5000 situated in the labs. The first beam was loaded in increments of about 0.2 mm / sec. The loading was continued until initial cracking of the beam occurred. At this point, the load was recorded, cracks were marked and noted. From initial cracking on the control beam, it was then observed until failure of the cracking patterns that were forming and crack widths were also noted. The control beam was then loaded to failure and removed.

Beam 2 was therefore the prestressed beam for  $A = 1\text{m}$ . Beam 2 was then loaded in

the exact manner as Beam 1, and loaded un-prestressed to the initial cracking load. At this point the load was removed from the beam and the residual deflection noted, with the cracks that formed. At this stage the prestressing apparatus is then applied, achieving 80 kN prestress in each cell making a total of 160 kN initial prestress. With the prestress applied, crack patterns were noted. With the anchorage plates, load cells and prestressing bars all connected to the beam, the load was then re-applied. From this stage the beam was again loaded until failure with all loads, deflections and observations being recorded.

The above procedure was then repeated for the 2nd loading position of  $A = 0.5\text{m}$ , for Beam 3 and Beam 4. This required the changing of the cross beam attached to the large hydraulic ram.

### 4.3 Formwork Construction and Details

The formwork required for this project consisted of light pine and ply-wood panels. Given the limited resources and laboratory space, the formwork was created with all four beams able to be formed in a single pour and housed within one set of formwork. This was efficient and was used for other students tests which were carried out. The form was constructed in the University of Southern Queensland Z101 workshop by a qualified carpenter. All measurements were given in detailed drawing and double checked as to meet the specimen design specifications.

The specifications that were required of the formwork to effectively house the beam specimens are listed below:

- The formwork was required to be strong enough to withstand the lateral loads and pressures caused from the beams during pouring, but more importantly during the removing of the beams.
- The formwork was strong enough to withstand the dead and live loads induced during the concreting process, from pouring to the fully set beams.
- Formwork durable and rigid enough for re-use.



- Formwork can be easily assembled and dismantled for the requirements of other students and moving the formwork around.
- Floor is stiff enough to prevent any sagging.
- Braces were enough to hold the dividing panels in their required positions during the pour, where when the bays were over half filled, the braces could be removed.
- Formwork was cheap and economical for construction and maintenance.
- At either end of the bays for each beam was a template made end piece that housed the ferrules during the pour. This piece was designed to place the 4 ferrules that will later attach the anchorage plate.

The formwork that was constructed was made from 12 mm ply-wood panels. The plywood was used for the floor, dividing panels and general boarding of vertical barriers separating the beams. The general frame and bracing of the formwork was constructed from pine joists and bearers as shown in Figure 4.1 below. Also the horizontal pine beams support the dividing panels was achieved by 3 pine pieces with supports at intervals to maintain the beam depth.

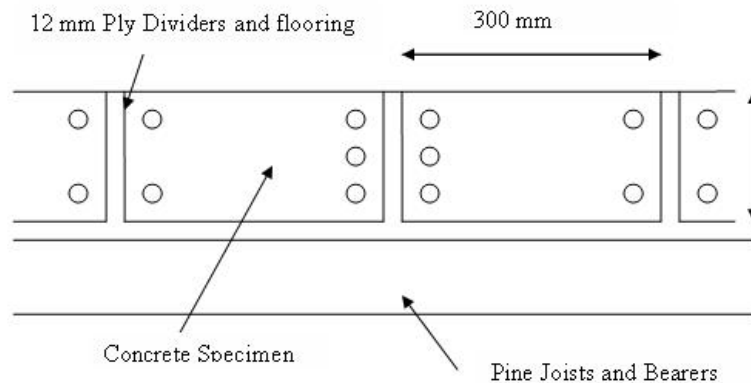


Figure 4.1: Section View of the Beams Formwork

All joints within the concrete pouring area of the formwork were filled with silicon, as to prevent the concrete from filtering between the dedicated bays. This was also used to prevent the filtering of water from the beams during the time within the formwork. Before the pouring of the concrete, all panels that were to come into contact with the



Figure 4.2: Completed Formwork



Figure 4.3: Completed Formwork

concrete were covered in grease to prevent the concrete adhering to the surface of the panels for ease of removal. The formwork was constructed in such a way that with the side bracing removed; the beams could be accessed and removed from a single side. That way the weight of the beams themselves could act against the suction formed when removing the beams.

#### 4.4 Steel Reinforcement Details

The preparation of the steel reinforcement cages of the test beams was again undertaken in the USQ Z101 laboratory. The laboratories proved most sufficient for the purposes of this project. Some of the major tasks that were undertaken in the preparation of the steel reinforcing cages can be seen below:

- Tension and Compressive, N12 steel reinforcement cut to the required length.

- The cutting and bending of the N6 shear reinforcement ligatures.
- The tying of the shear ligatures at the required spacing to the compressive and tension reinforcement to create the required section.
- The cutting bending and attachment of the lifting points.
- Placement of the ferrules reinforcement.
- Surface preparation to the steel reinforcement where strain gauges were to be placed, involving the use of a grinder, file and emery paper.

The length of the compression and tensile reinforcement remained consistent throughout all the four beams. The steel was cut to 3460 mm, where 20 mm cover was left on each of the bars to the end of the beam. The shear ligatures were all bent by hand on a custom made jig (Figure 4.4) to maintain the 25 mm cover and fit the section. The completed reinforcing cages were all tied by hand.

A total of 21 shear ligatures were required for each individual reinforcing cage, therefore for the 4 beam specimens, a total of 84 shear reinforcing ligatures were required. The spacing for the shear ligatures can be seen from section 3.3.2.

The reinforcing cages were constructed by hanging the top flexural reinforcement on a wooden stand that was clamped to a desk. The shear ligatures were slid into positions and put in their general spacing which was marked along the flexural reinforcement with a marker. The shear reinforcement was then tied to the flexural reinforcement. The bottom flexural reinforcement was then slid into the shear ligatures and positioned correctly. Then maintaining a square cage, the remaining ties were tied to complete the reinforcing cage. Once the cages were completed (Figure 4.5), the lifting hooks were then tied into the shear ligatures on the underside of the reinforcing cage. The lifting points were designed at specific locations so that when the beams were lifted from the formwork and transported no failure or induced cracking occurred. These locations existed 750 mm from either end of the beams, and 2000 mm between them.

The completed reinforcing cages with the lifting hooks and all strain gauges attached were then lifted and placed within the completed formwork. Here the cages were set in



Figure 4.4: Custom Jig

position with reinforcing chairs at the required cover of 25 mm. The chairs were placed on either side and underneath the reinforcement to maintain the cover as the concrete was poured and compacted. As shown in Figure 4.6 the cages have been placed within the formwork, and all reinforcing chairs placed. It can also be seen that the strain gauges were placed in plastic bags to protect them throughout the pouring and curing of the concrete.

As seen in Figure 4.6 the chairs can be seen on the sides and beneath the reinforcing cages to maintain cover of the concrete over the reinforcement.



Figure 4.5: Completed Reinforcing Cage

## 4.5 Concreting

Ready mix concrete from local supplier within Toowoomba, were used for the acquisition of concrete for the purpose of this project. The concrete was specified at 40 MPa concrete and with a maximum aggregate size of 20 mm. A slump test of the concrete was carried out on site before the concrete was poured; a slump of about 75mm was achieved and was a suitable workability for the purpose of pouring the beams. Also on the day of pouring, a total of 4 concrete cylinders per beam were poured. These cylinders were later used to confirm the concrete compressive strength, but more to give an indication of the concrete compressive strength on the day that each beam was tested. The concrete cylinders along with the beams were not cured in a fog room, as they proved to large and hard to manipulate into such a room , rather all test specimens were placed outside under large sheets of plastic, where water was applied every second day where practical.

Some of the major tasks that were undertaken in the preparation of the steel reinforcing cages can be seen below:



Figure 4.6: Steel Reinforcing Chairs

- During concrete pouring all strain gauges were bagged and sealed as to not be damaged.
- All formwork was greased prior to pour.
- All concrete works were done immediately before the concrete set.
- The pine separators used to maintain the concrete beam depths was checked to be firmly secure as to not move during the pour.
- All chairs and reinforcement positions were checked.
- The concrete was compacted using a machine operated vibrating machine. This machine enabled that the required compaction was achieved, and no voids were left in the beams which could impede the beams strength or create areas where stress concentrations may form.
- All works were carried out under supervision and safety equipment was used.

As shown in Figure 4.7 above, the concrete was hand finished and cast level to the top of the formwork. Again you can see the strain gauges housed within the plastic bags.



Figure 4.7: Completed Cast Concrete

These photos demonstrate how the beams reside in the formwork, where they all lay on the deepest part of the section base to base. When removing the beams, the side bracing was removed and each beam was taken by a forklift from the one side. As a beam is being removed the self weight of the other beams acts as a dead weight.

As can be seen in Figure 4.8 the concreting required the concrete moulds to be filled. All moulds were greased heavily for ease of removal. Four cylinders were used for each beam. As also can be see, the large cylinders were used for an indirect tensile test, where one cylinder existed for each beam. The smaller cylinders used for the compression testing of the concrete were 100 mm in diameter and 200 mm high. The larger cylinders were 150 mm in diameter and 300 mm high. The smaller cylinders were cured exactly the same as the larger beams and on the day of testing, a compression test was carried out using the Avery Testing Machine at Engineering Z101 laboratory (shown in Figure 4.9). All safely precautions and skilled operators were present in the testing of these cylinders.



Figure 4.8: Coompression Testing Cylinder Moulds

## 4.6 Instrumentation

All instrumentation involved in this project was dedicated to the measuring of:

- Strain in internal steel
- Strain in the external concrete
- Deflections
- Load
- Load in external prestressing tendons
- Crack widths

Therefore the major instrumentation involved the placement of:

- 2 mm strain gauges on the internal steel reinforcement
- 30 mm strain gauges on the external concrete





Figure 4.9: Compression Testing of the Concrete Cylinders in the Avery Machine

- Load Cells
- Linear Variable Displacement Transducer (LVDT)

The strain gauge data sheets have been included in Appendix B for specific details entailing to there specifications.

Shown below in Figure 4.10 is the testing system used for all experimental testing in this project.

#### 4.6.1 Strain Gauge placement

The placement of the 2 mm strain gauges on the steel reinforcement was briefly discussed in section 4.4. The strain gauges were placed on the internal steel reinforcing cage in the early stages of the specimen preparation. Each reinforcing cage required the placement of 5 x 2 mm strain gauges. Three strain gauges were placed on the flexural steel reinforcement and two strain gauges were placed on the shear reinforcement. The flexural steel strain gauges were placed at mid-span, as this is the critical section of



Figure 4.10: Testing System including Prestressing and the System 5000

the flexural stresses. Of the three strain gauges, two were placed on the tensile reinforcement and a single gauge was placed on the compression reinforcement. The strain gauge that was placed on the shear reinforcement was placed on the shear ligature that resided 800 mm from mid-span, in both directions. This strain gauge was placed in the area where the shear was critical, as the shear cracks and thus the largest shear force acts from the supports a distance  $D$ , equal to the depth of the beam up to the point of contact with the point load. All strain gauges that were placed on the steel reinforcement were placed on a prepared surface that had been ground flat and cleaned using acetone. Wax and waterproof tape were then applied to the strain gauges to seal them from coming in contact with the water that resides within the concrete which could cause a short circuit.

As can be seen in Figure 4.11, the 3 strain gauges placed on the flexural steel were labelled TF for the top flexural reinforcement, and then BF1 and BF2 respectively for the outside bottom flexural reinforcement.

The external concrete strain gauges were placed at mid-span of the concrete beam. Five 30 mm strain gauges were used. Two gauges were placed on the top side of the

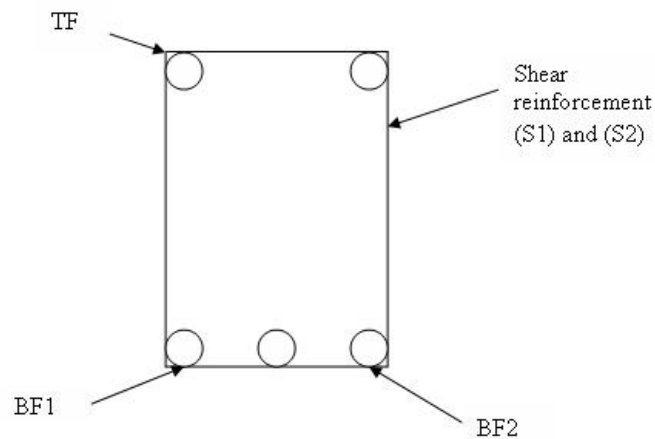


Figure 4.11: Labelling of the Flexural Steel Strain Gauge

concrete beams surface and then three were placed running vertically positioned about a third of the depth between them. The concrete strain gauges were required to bond with the concrete, to achieve this, the following process was undertaken:

- Cleaning of the surface area with a steel brush.
- Sanding the area with sand paper
- Cleaning the concrete area with acetone.
- Application of a polyester adhesive (bonds the strain gauge, with no effect from moisture , temperature or voids)
- The adhesive was given a day to dry and harden.
- The strain gauge was then applied to the prepared region.

As shown in Figure ?? the 30 mm strain gauges are situated in the central region of the surface prepared with the adhesive in the process described above.

All strain gauges were tested using a multimeter (Figure 4.12) to check if the bond had been achieved correctly before continuing with the testing. Shown below in Figure 4.14 is the numbering and general placement of the concrete 30 mm strain gauges.



Figure 4.12: Application of Shear Reinforcement Strain Gauges

#### 4.6.2 Linear Variable Displacement Transducer (LVDT) Placement

The LVDT was placed at the mid-span of the test beams, as this is where the maximum deflection will occur. The LVDT will measure and feed back to the system 5000 the vertical displacement or deformation of the concrete beam under loading. As can be seen in Figure 4.15 a small steel plate was attached to the underside of the concrete beam. The LVDT then rested on the top surface of the plate, which is equivalent to the bottom surface of the concrete beam. As the beam deflects the LVDT's rod will displace and the measurement is recorded in mm in the computer.

#### 4.6.3 Load Cells and Anchorage Apparatus

The load cells were required in the testing phase to measure the axial force within the external prestressing bars. The cells were required to achieve the required initial prestress as the hydraulic jack induced the compressive force in the rods. Also the cells were required throughout the testing to monitor the axial load in the prestressing tendons as the beam underwent loading and deflected.



Figure 4.13: Multimetre, Adhesive and Acetone

Figure 4.17 also depicts the anchorage of the load cell end of the test specimen. As can be seen in the photo, the large steel plate held in place by the cast in ferrules sits flush with the base end of the beam. The plate had two holes situated either side for the external bars to be inserted. Then through a series of anchorage plates at the front and base of the cells and rod, the nuts on the threaded bars could then be tightened to achieve the compressive force.

Figure 4.17 and 4.18 give an indication for the jacking system which was used to apply the initial prestress. The hydraulics were hand operated and monitored at the computer via the outputs of the load cells. The jack would induce a compressive force in the tendon under stressing force, then by tightening the nut that resides within the central region of the jack, the stress could be maintained and the jack removed. The system allowed for little slip or loss of prestress and proved very effective for the purposes of the project. The tendons were stressed simultaneously; increasing the stress in each bar by small increments until the load of 80 kN was achieved. This was done for safety purposes.



Figure 4.14: Top Concrete Strain Gauges

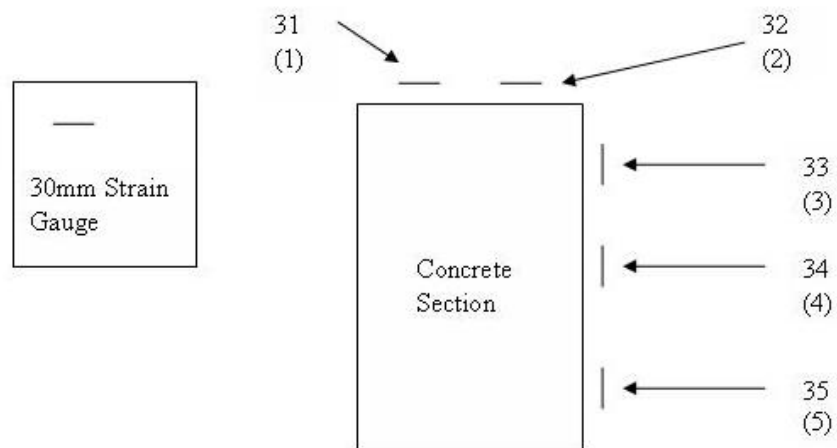


Figure 4.15: System 5000 Strain Gauge Data Lines



Figure 4.16: LVDT



Figure 4.17: Load Cells in Position for Initial Prestressing





Figure 4.18: Hydraulic Jack and Prestressing Apparatus



# Chapter 5

## Results and Discussion

### 5.1 Introduction

This chapter will discuss the results that were obtained through the testing or experimental phases of the project. This chapter will also include a section that analysis the theoretical predictions with the actual experimental results. A discussion on the experimental outcomes in relation to real life in service applications will be undertaken. The results will include all experimental results obtained in the following tests:

- Compression testing of concrete cylinders
- Flexural testing of control beam
- Flexural testing of the prestressed beam

Four main sets of results exist for the flexural testing. Two sets of data for the control beam at  $A = 1$  m and  $A = 0.5$  m and then another two sets for the prestressed beams at  $A = 1$  m and  $A = 0.5$  m.

Initially the chapter will discuss the compression testing results, resulting in the design specimens compression strength. The results obtained through the physical testing of the control beams will be discussed first. These results support the flexural strength

Table 5.1: Strain Gauge Labels and Relevant System 5000 Input Lines

Strain Gauge	System 5000 Data Line
1 (concrete)	31
2 (concrete)	32
3(concrete)	33
4 (concrete)	34
5 (concrete)	35
S1 (steel)	36
BF1 (steel)	37
TF (steel)	38
S2 (steel)	39
BF2 (steel)	40

of the concrete section under the defined loading positions. The results for the two prestressed beams will follow, where the flexural strength of the prestressed beams will be discussed. Following these two sections the loading position and theoretical versus experimental results sections will also be introduced. This chapter will also discuss the increase in prestressing force and look at some of the strains within the concrete.

The testing data that was recorded by the system 5000, including all strain and forces applied to the beams have been included in Appendix C. These are the data sets as outputted from the system 5000 system. The strain gauge readings, load cells and deflections are all recorded within these data sheets.

For the purpose of all the test data in the Appendix C, each column represents a different reading. Shown below in table 5.1 are the relevant readings recorded during testing to the labels of the connections lines in the system 5000. The table shows which strain gauge positioned on the steel and concrete is the relevant label to the input lines into the system 5000.

It should be noted that in understanding the graphs shown throughout the results section, the far end of all the graphs reach a maximum points then seem to arch back towards the starting position. This is explained easily, as when the load is removed

Table 5.2: Compression Test Results

Cylinder	1	2	3	4	Avearge	$\varepsilon$
	(kN)	(kN)	(kN)	(kN)	(kN)	(MPa)
Test 1	305	327	307	310	309.25	39.44
Test 2	308	295	309	317	307.25	39.12
Test 3	302	310	300	305	304.25	38.7
Test 4	315	310	300	307	308	39.22

form the beams, the load then decrease, and the deflection decreases. The curve will not return to the original position as steel has been loaded passed its elastic limit and plastic deformation has occurred. Thus a residual deflection will remain. It is evident that this residual is larger in the control beams compared to the prestressed beams, as the prestressed beams then have the axial force induced from the prestress to aid the recovery of the beam.

### 5.1.1 Compression Testing Results

This subsection will discuss the results obtained on the compression testing on the concrete cylinders. The concretes strength from the compression testing was used for the calculation of the concretes strength for each beam, as the compression tests were carried out on the day that the test beams were tested, approximately 4 cylinders for each beam.

It can be seen in Table 5.2 that for each test, which in-fact corresponds to each beam (e.g. Test 1 = Beam 1), 4 cylinders were tested, and averaged to give a good indication of the concretes compressive strength on the day of testing.

The force recorded from the Avery Machine in the laboratory is easily converted to the Compressive strength of the concrete, as shown below:

For a simple cylindrical shaped cylinder, The compressive stress in the concrete is given as,  $\varepsilon_s = \text{Force} / \text{Cross-sectional Area}$  ( $\varepsilon_s$  in MPA)

Therefore given the results, it was seen that the concrete was close enough to being assumed 40 MPa which had been used in the calculations, therefore was not changed or any calculations corrected.

### 5.1.2 Flexural testing of Control Beams

The first control beam that was tested was Beam 1, which was the control beam for the loading position of  $A = 1$  m. The results can be best shown in graphical format, as shown below in Figure 5.1.

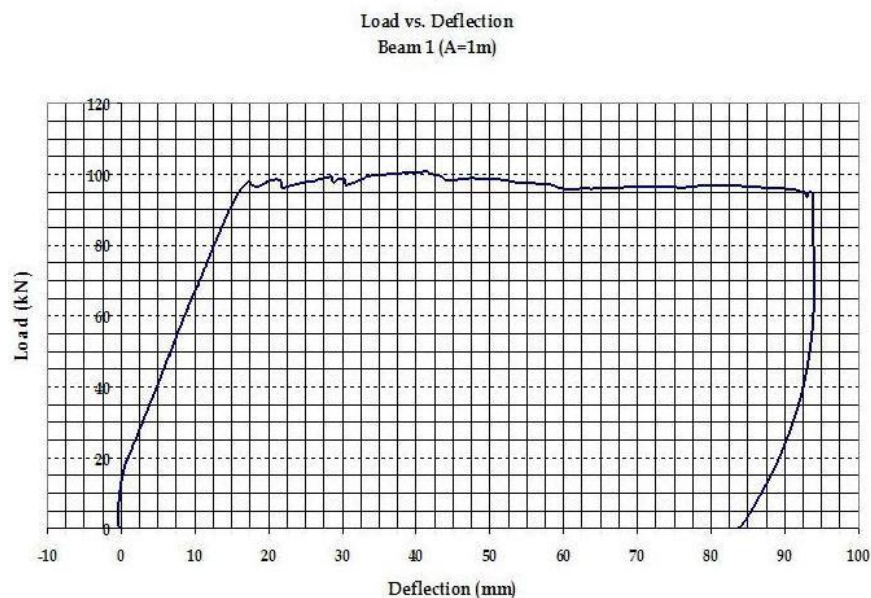


Figure 5.1: The Load versus Deflection for Control Beam 1

Therefore it can be seen for the control beam of the loading position of  $A = 1$  m, the ultimate force achieved to fail the beam in flexure was 100.73 kN with a maximum deflection of 93.86 mm. During the testing the beam was observed to initially crack at about 25 kN, which can be seen in the on Figure 5.1 at about 20 kN where the slope of the curve decreases.

As the load increased to about 32 - 40 kN small flexural cracks mid-span and either side of the loading points formed. Between the loads of 52 - 66 kN these existing flexural cracks lengthening and begun to widen to about 0.2 mm. There was new evidence of

new flexural cracks forming along the bottom span of the beam from about half way to where the point load is applied to the support either ends. At about 75 kN the cracks below the loading points began to widen to about 0.5 mm and 0.3 mm in width. Even with the entire shear reinforcement and checking of shear strength, understanding that the beam was highly compensated for shear failure, at 75 - 85 kN shear cracks formed on either end of the control beam. They formed where predicted, about distance  $D$  away from support and propagated up to the point load application point. These shear cracks were hairline cracks that formed, but then did not advance or change throughout the remaining loading cycle. When the load reached about 98 kN the flexural cracks that existed mid-span of the beam began to really widen, shown in Figure 5.2 where the cracks reached a width of about 2-4 mm. About this stage of loading, between 96 and 98 kN, the concrete crushed on the compression side of the beam, this occurred at about 60 - 70 mm deflection.

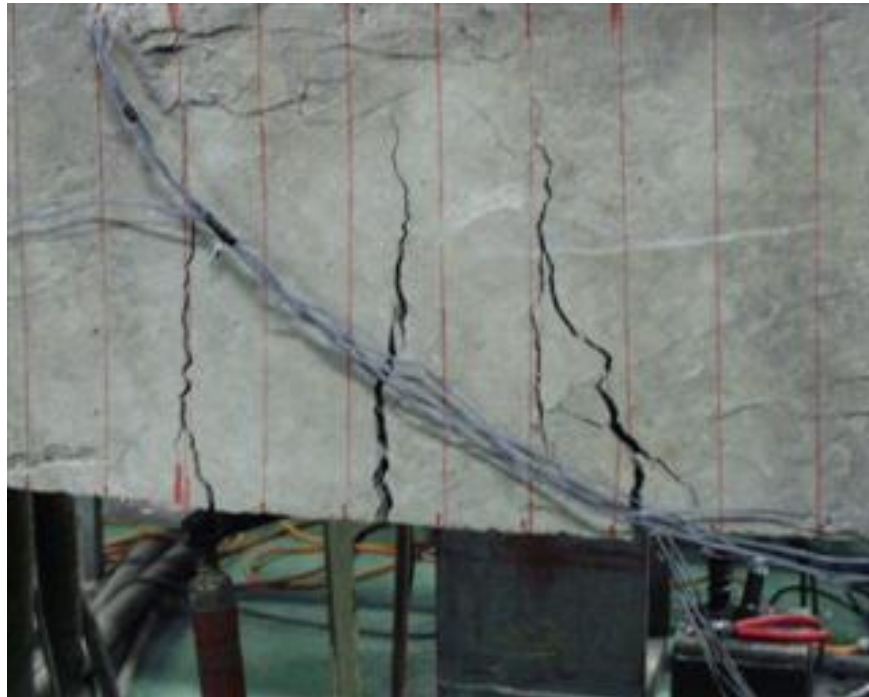


Figure 5.2: Mid-Span Flexural Cracking of the Control Beam

The second control beam, Beam 3 at  $A = 0.5$  m was tested. The results are again shown in graphical format below in Figure 5.3.

Therefore it can be seen for the control beam of the loading position of  $A = 0.5$  m,

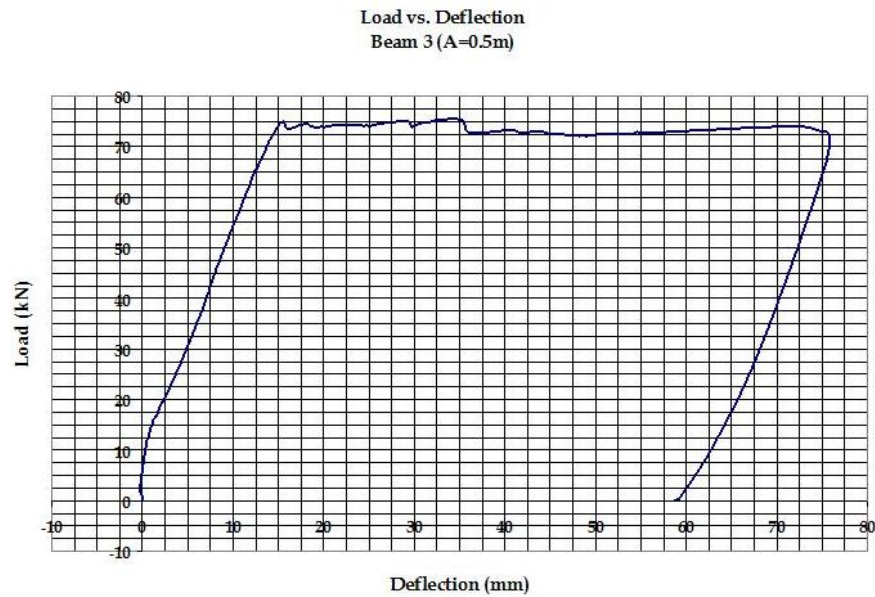


Figure 5.3: Load versus Deflection for Control Beam 3

the ultimate force achieved to fail the beam in flexure was 74.09 kN with a maximum deflection of 75.84 mm.

The initial cracking of this control beam was observed to occur at about 16 kN, which again can be seen in Figure 5.3 where the curve decreases in slope at about 15 kN. The initial cracking started with a hairline crack forming mid-span. At about 19 -20 kN the cracking had progressed to hairline cracks again forming mid-span and on either side of the loading points. This pattern was similar to control beam for the loading position of  $A = 1$  m. Then from about 26 kN through to about 55 kN the existing flexural cracks propagated to the neutral axis depth of the concrete section and new flexural cracks along the span were formed. Then as the steel reinforcing began to yield and the deflection increase, at about 74 kN the flexural cracks were visible and were about 1 mm in width. As the loading continued large cracks of about 2- 3 mm formed mid-span and also under the loading points. Local crushing of the compressed concrete occurred at about 74 kN, as shown in Figure 5.4, with a deflection of about 40 mm.

Therefore compared to the first control beam that with a loading span of 1m shear cracks initially formed but did not propagate, continuing to fail in flexure, the second control beam did not have any shear cracks forming, due to the tighter span width



Figure 5.4: Local Crushing of the Concrete Mid-Span of the Beam

of the loading positions. Though the other crack patterns were very similar, the first beams final cracks were largest mid-span, whereas the second beams final crack patterns remained with the cracks beneath the loading points at maximum width.

### 5.1.3 Flexural testing of Prestressed Beams

The first prestressed beam that was tested was Beam 2, which was the prestressed beam for the loading position of  $A = 1$  m. The results can be best shown in graphical format, as shown below in Figure 5.5.

Therefore it can be seen for the prestressed beam of the loading position of  $A = 1$  m, the ultimate force achieved to fail the beam in flexure was 151.46 kN with a maximum deflection of 34.56 mm.

In this test as can be seen in Figure 5.5 there is a smaller loop within the larger loop. This loop exists as to prestress the concrete beams which exist in service and to achieve results which are applicable in service, the beam must be cracking and the steel begun

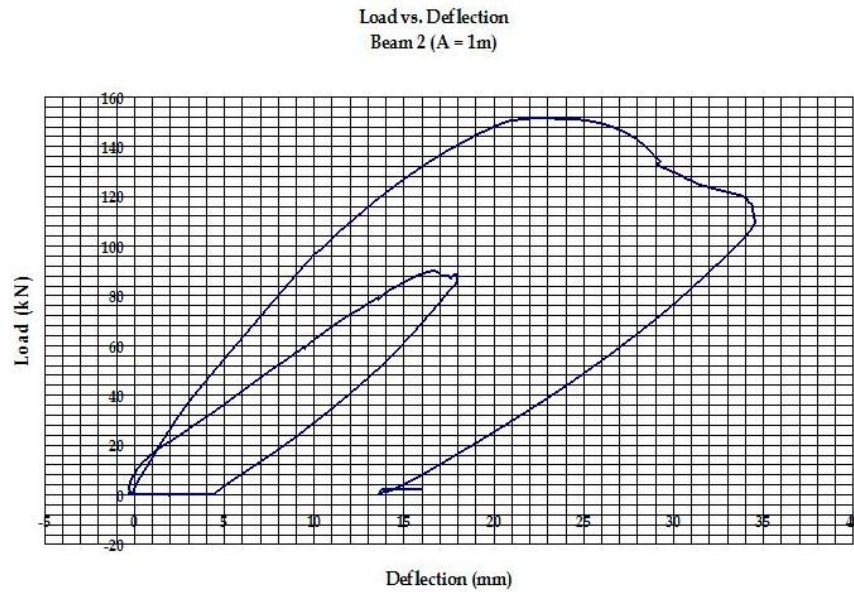


Figure 5.5: Load Versus Deflection for Prestressed Beam 2

to yield, where a residual in the deflection of the beam exists. Therefore that smaller loop is the loading of the beam to initial yielding of the steel. Later in this chapter it can be seen that the smaller loops generally match up with the control beams curve, this occurs as it is where the steel begins to yield. It was noted from observations initial cracking of the un-prestressed beam, with loading position of 1m was at about 22 kN. The initial cracking consisted of hairline flexural crack mid-span. At about 27 kN, these flexural cracks began to form along the length of the span of the beam, again from loading point to loading point. The reaction of the un-prestressed beam to the loading again continued with general propagation of the cracks, widening and some new cracks forming up to about 85 kN. The flexural cracks were about 0.3 - 0.5 mm wide. The deflection at this stage was about 18 mm. The cracking patterns of this beam were in-fact very similar to the initial testing of the control beam as expected, even the same shear cracks formed in almost identical positions. Note that at the point of removing the load, a 4.3 mm residual deflection remained in the beam from the yielding of the steel. All cracks were marked with a pencil and the position marked, for comparison on completion of the testing. After the prestress was applied, it was noted that no cracking was easily visible and all cracks were deemed to be closed. This is caused from the induced moment from the prestress which acts against the self weight of the beam.



The load was then re-applied to the beam after prestress. No cracks were visibly opening or forming until about a 90 kN load had been applied, where the flexural cracks mid-span and around the loading points were becoming more visible. At about 110 kN it was evident again that the cracks were opening up and again propagating. This was especially evident in the mid-span flexural cracks. At 155 kN, a new shear cracked formed, parallel to the existing shear crack that by this stage still had not formed a dominant crack, but remained about the same width throughout the test. Not long after the 155 kN mark was reached, the compression concrete was crushed. All flexural cracks did not exceed 1 - 2 mm at the final load and deflection. After the testing a residual deflection of about 13 mm remained (can be seen as the difference in the starting and finishing of the prestressed curve, the two x intercepts of the larger curve). Therefore after the first part of the test, a 4 mm residual remained which means that the residual increase by about 8 mm after the prestressing loading had been removed.

The second prestressed beam, Beam 4 at  $A = 0.5$  m was tested. The results are again shown in graphical format below in Figure 5.6.

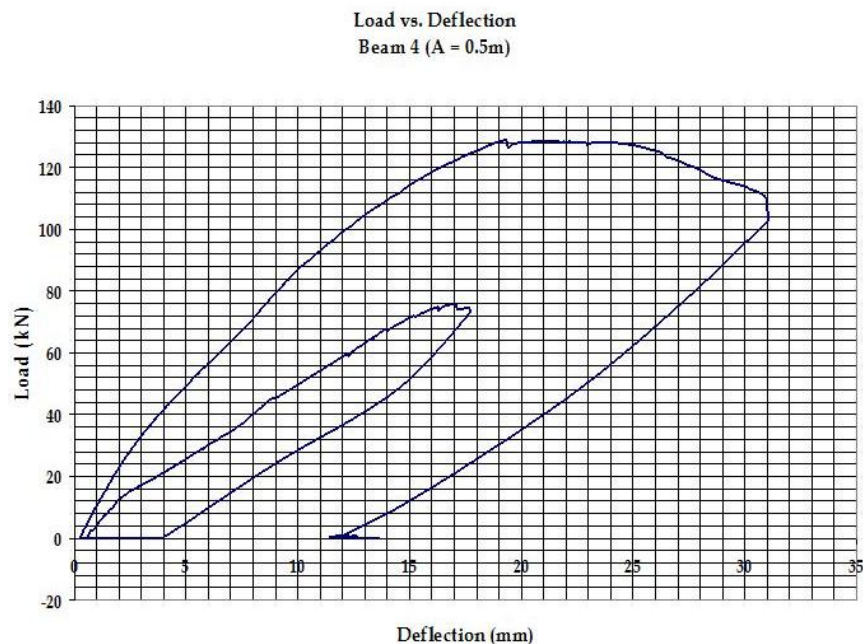


Figure 5.6: Load Versus Deflection for Prestressed Beam 4

Therefore it can be seen for the prestressed beam of the loading position of  $A = 0.5$  m,

the ultimate force achieved to fail the beam in flexure was 128.94 kN with a maximum deflection of 31.04 mm.

In this test as can be seen in Figure 5.6 there is a smaller loop within the larger loop. This loop exists as to prestress the concrete beams which exist in service and to achieve results which are applicable in service, the beam must be cracking and the steel begun to yield, where a residual in the deflection of the beam exists. Therefore that smaller loop is the loading of the beam to initial yielding of the steel. Later in this chapter it can be seen that the smaller loops generally match up with the control beams curve, this occurs as it is where the steel begins to yield. It was noted from observations initial cracking of the un-prestressed beam, with loading position of 0.5 m was at about 21.5 kN. The initial cracking consisted of hairline flexural crack mid-span. At about 38 kN, these flexural cracks began to form along the length of the span of the beam, again from loading point to loading point. The reaction of the un-prestressed beam to the loading again continued with general propagation of the cracks, widening and some new cracks forming up to about 75 kN. The flexural cracks were about 0.5-1 mm wide. The deflection at this stage of loading was about 17 mm. The cracking patterns of this beam were in-fact very similar to the initial testing of the control beam as expected, though this time shear cracks formed on the initial loading, where on the control beam they did not. Note that at the point of removing the load, a 3.6 mm residual deflection remained in the beam from the yielding of the steel. All cracks were marked with a pencil and the position marked, for comparison on completion of the testing. After the prestress was applied, it was noted that no cracking was easily visible and all cracks were deemed to be closed. This is caused from the induced moment from the prestress which acts against the self weight of the beam.

The load was then re-applied to the beam after prestress. No cracks were visibly opening or forming until about a 57 kN load had been applied, where the flexural cracks which existed below a loading point opened quite significantly in relation to the other flexural cracking. It was noted that this crack was a significant crack in the initial loading of the beam. At about 73 kN it was evident again that the cracks were opening up and again propagating. This was especially evident in the mid-span flexural cracks. Though at this stage no new cracks had formed, that were visibly accessible. It was

also noted that the shear cracks remained closed. At 95 kN, the large flexural cracks were easily visible and were of a width of about 1 mm. Not long after the 105 kN mark was reached, new flexural cracks begun to form on the underside of the beam. At about 122 kN the shear cracks again became visible, but did not propagate. At 128 kN, it was discovered that new shear cracks again formed. The crack appeared with a more acute angle to the base of the beam than the existing shear cracks and closer to the loading point. At about 126 kN the compression concrete was crushed, and cracks between 1- 2 mm were observed. After the testing a residual deflection of about 11.5 mm remained. Therefore after the first part of the test, a 3.6 mm residual remained which means that the residual increase by about 8 mm after the prestressing loading had been removed.

#### 5.1.4 Control Beams versus Prestressed Beams

This subsection will discuss the control beams results superimposed with the prestressed results for each beam respectively. Again all data for the prestressed beams and control beams can be found in Appendix A. With the graphs superimposed on each other the strength increase and deflection decreased accompanying the prestressed beams can be easily seen.

The results for the loading position of  $A = 1$  m can be shown below in Figure 5.7, where the prestressed results have been superimposed with the control beams results

As can be seen in Figure ??, the prestressed results have been superimposed on the control beams results for the loading position of 1 m. As stated in the previous section you can see that the smaller loop of the prestressed graph almost matches with the curve on the control beam. This represents that the prestressed beam was attempted to load to a point of yielding, where cracks and a residual deflection would exist. It can easily be justified that the prestress increases the strength quite dramatically; where the maximum flexural load of the control beam was about 100 kN compared to the prestressed beam of about 151 kN. But most noticeably decreases the deflection of the beam by a considerable amount, where the max deflection of the control beam was 94 mm, compared to the maximum deflection of the prestressed beam which was 34 mm.

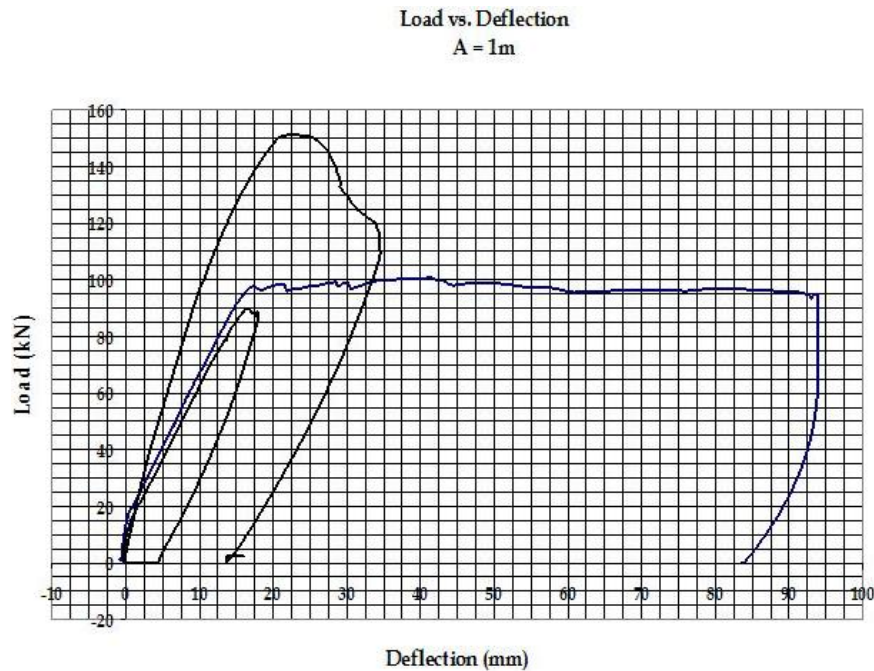


Figure 5.7: The Load versus Deflection for the Control Beam and Prestressed Beam of Loading Position of  $A = 1\text{m}$

The results for the loading position of  $A = 0.5\text{ m}$  can be shown below in Figure 5.8, where the prestressed results have been superimposed with the control beams results.

As can be seen in Figure 5.8, the prestressed results have been superimposed on the control beams results for the loading position of  $0.5\text{ m}$ . As stated in the previous section you can see that the smaller loop of the prestressed graph is very close to match with the curve on the control beam. This represents that the prestressed beam was attempted to load to a point of yielding, where cracks and a residual deflection would exist. It can easily be justified that the prestress increases the strength quite dramatically; where the maximum flexural load of the control beam was about  $75\text{ kN}$  compared to the prestressed beam of about  $130\text{ kN}$ . But most noticeably decreases the deflection of the beam by a considerable amount, where the max deflection of the control beam was  $75\text{ mm}$ , compared to the maximum deflection of the prestressed beam which was  $31\text{ mm}$ .

Table 5.3 below shows the percentage increase achieved by the prestressing force on the control beams. This gives an indication of the expected flexural increase in the beams strength if these prestressing techniques are applied. Also shown in Table 5.4 is the decrease in the maximum deflection achieved by the prestressed beam in comparison

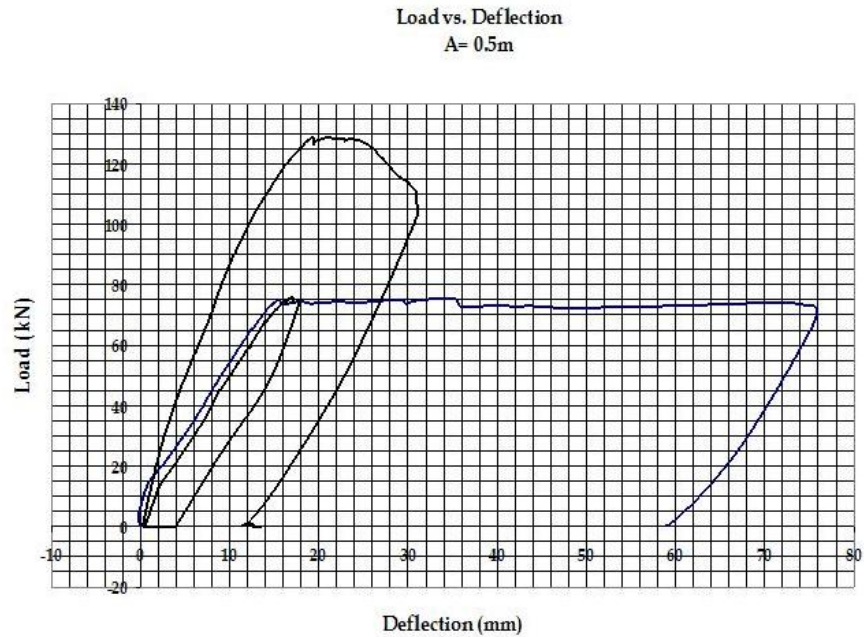


Figure 5.8: The Load versus Deflection of the Control Beam and Prestressed Beam for Loading Position of  $A = 0.5\text{m}$

Table 5.3: Percentage Increase in Flexural Strength after Prestress

Loading Position	Control Beam	Prestressed	Increase	% Increase
	(kN)	(kN)	(kN)	
$A = 1\text{ m}$	100.73	151.46	50.73	50.04%
$A = 0.5\text{ m}$	74.09	128.94	54.85	74.03%

with the control beam. Therefore given a simply supported flexural member in service in similar loading conditions, the increase in flexural strength and decrease in deflections could be expected to be similar to the results shown in these tables.

## 5.2 Comparison of Loading Position

This subsection shows how the variance in loading position has altered the strength and deflections of the experimental results. This section will describe the difference in strength and deflections and crack patterns that were established on the variation in loading position. The variation in loading positions have been describe quite thoroughly

Table 5.4: Percentage Decrease in Deflection after Prestress

Loading Position	Control Beam	Prestressed	Decrease	% Decrease
	(kN)	(kN)	(kN)	
A = 1 m	93.86	34.56	59.3	63.18%
A = 0.5 m	75.84	31.04	44.8	59.07%

but for the sake of clarity, the two loading positions analysed was a distance of 1 m and 0.5 m between point loadings.

The comparison between the two control beams and the two prestressed beams can be seen in graphical format. Shown below is the comparison of the control beams in Figure 5.9.



Figure 5.9: The Load versus Deflection for the Control Beams

It can be seen that for the loading position of 1m, Beam 1 the maximum load achieved was about 100 kN compared to the maximum load of the 0.5m, Beam 3 which achieve about 75 kN maximum load. This variance occurs in accordance with the theory, where the further the load is away from the mid-span towards the supports, to fail the beam in flexure, the force required increases. Thus the close the point loads spacing becomes

to exist as a point load, the less amount of force required to fail the beam in shear.

The the force required to fail the 1m loading position is greater than the 0.5 m position as the closer the spacing the less force required, and the further the spacing, towards the supports, the greater the force required. The prestress does not alter this fact, but just increase the amount of load required to fail the beam in flexure.

Shown below is the comparison of the prestressed beams in Figure 5.10,

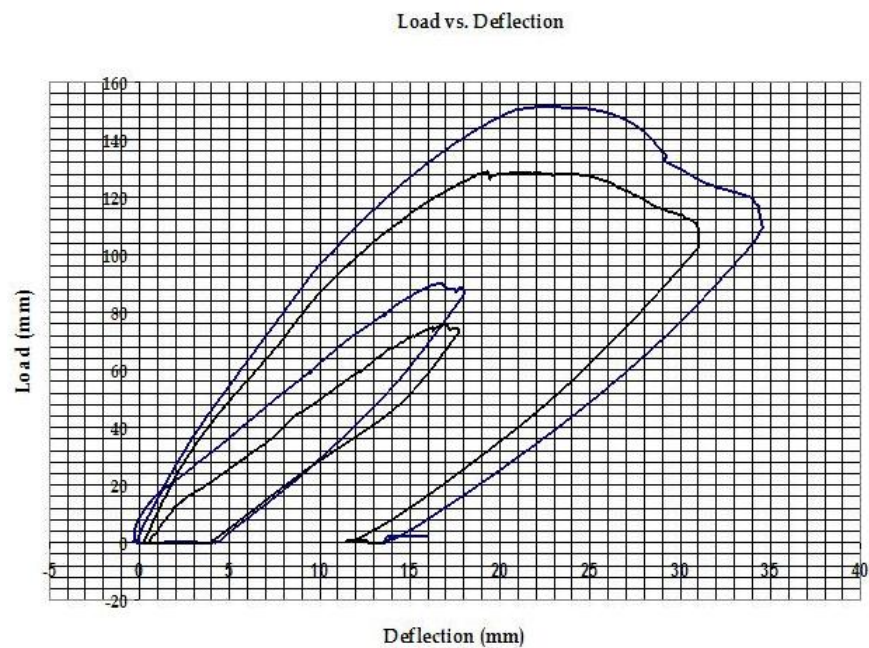


Figure 5.10: The Load versus Deflection for the Prestressed Beams

From the results some observations on the crack patterns throughout the testing have been made. These observations and comparisons have been listed below:

- All cracks were closed on both loading positions after the application of prestress
- Shear cracks did not form on the 0.5 m loading positions control beam, but did form on the prestressed beam. Though shear cracks formed on both the control and prestressed beam for the 1m loading position. Shown in Figure 5.11 is the shear cracks that were seen on all 3 beams, where the crack would start near the supports and propagate towards the point of loading.



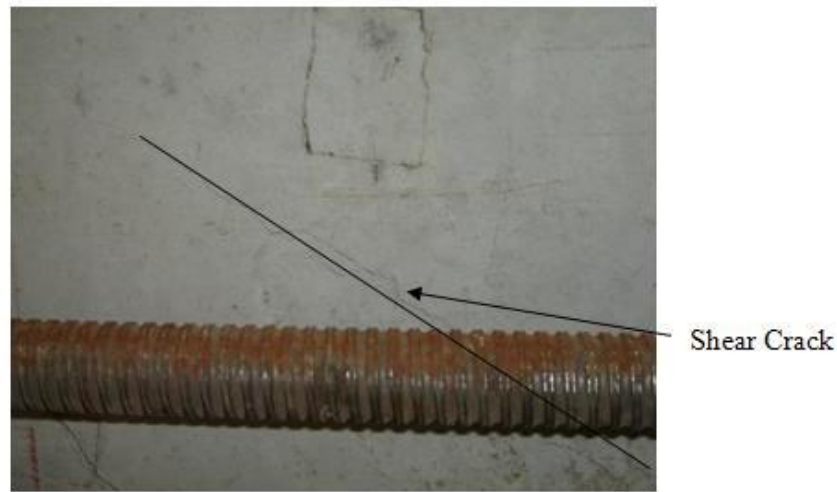


Figure 5.11: Propagation of the Shear Cracks Formed

- All cracks generally formed in similar patterns, where the first cracks would always form mid-span and directly either side of each of the loading positions shown in Figure 5.12 where the majority of major flexural cracks exists at mid-span and beneath the loading points.
- A large amount of the stiffness and rigidity of the section was due to the large diameter and stiffness of the prestressing bars. Though this affect has not been quantified.
- As the prestressing force closed all cracks, before overloading of the beams occurred, there may not be a need for crack repair methods, given the section is deep enough and the prestressing force is adequate. The closing of all the cracks after prestress also verifies the assumption of using the strength prediction equation for a “new section”, which is assumed to be un-cracked within this project. Having all cracks closed therefore enables the percentage increase in flexural strength.



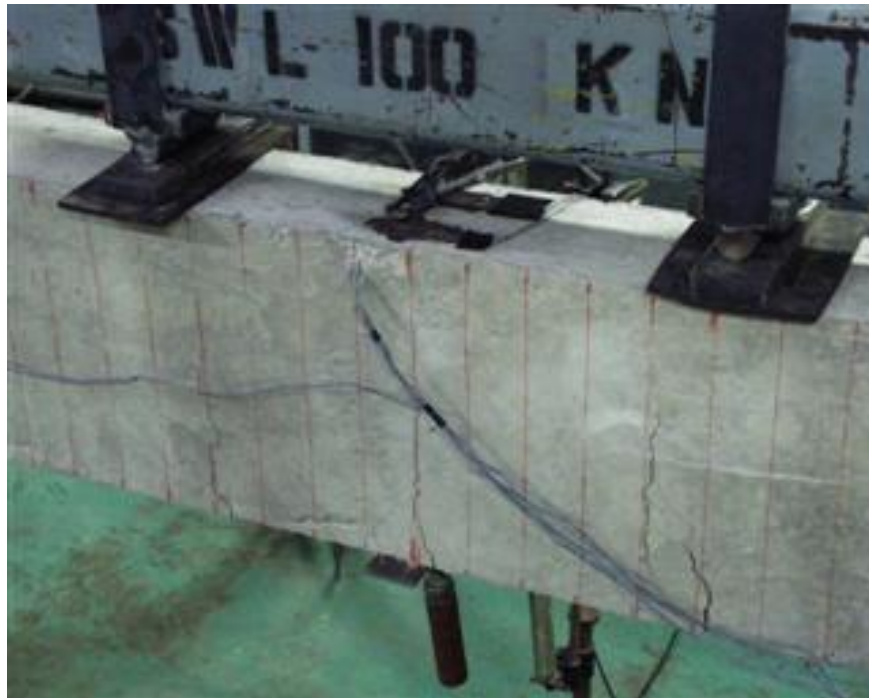


Figure 5.12: Typical Flexural Crackign Pattern for All Test Specimens

### 5.3 Theoretical versus Experimental Results

This subsection of chapter 4 will discuss how the experimental results achieved faired against the theoretical predictions that were made. The section will describe the percentage variance in strength that was found between the theoretical and experimental results.

Table 5.5 below shows the variance in the predicted force required to fail the control beam in flexure compared to the actual experimental results achieved. This gives an indication of the accuracy in the theoretical predictions to the actual experimental results achieved. Also shown in Table 5.6 is the variance achieved in the theoretical predictions of the maximum load required to fail the prestressed beam in flexure to the actual recorded values.

Tables 5.5 and 5.6 show some variance in the computations in the expected flexural strength to the experimental values. Some of the possible variance that could of lead to the difference has been thought to include the following:

Table 5.5: Theoretical versus Experimental Flexural Control Beam Results

Loading Position	Control Beam	Control Beam	Increase	% Increase
	(Theoretical)	(Experimental)		
	(kN)	(kN)	(kN)	
A = 1 m	81.45	100.73	19.28	23.7%
A = 0.5 m	65.16	74.09	8.93	13.7%

Table 5.6: Theoretical versus Experimental Flexural Prestress Results

Loading Position	Prestressed Beam	Prestressed Beam	Variance	% Variance
	(Theoretical)	(Experimental)		
	(kN)	(kN)	(kN)	
A = 1 m	134.32	151.46	17.14	12.8%
A = 0.5 m	107.45	128.94	21.49	20%

- The second order effects were not taken into account; this would have an effect especially mid-span of the beam where the eccentricity under large deflections would induce a moment which would detract from the positive effect of the prestressing force.
- The actual prestressing force within the tendons increased to larger values than the prestressing formula predicted. The theoretical prediction of the stress in the tendons with an initial prestress of 160 kN, resulted in a prestressing force of about 201.7 kN with the addition of the incremental stresses caused from the beam deflecting under the applied load. Whereas can be seen in Appendix C, for Test 2 (prestressed beam of 1 m loading position), the force within the tendons got as high as 259 kN (this is calculated by the addition of the force recorded in the load cells columns of the data sheet (labelled 8 and 9)). After manipulating the data, with the implementation of this extra recorded incremental increase in prestress, the theoretical expected ultimate force is much closer to the actual recorded values. A closer look at this is shown in section 5.4.
- The formulas are always conservative values, and would never be expected to exceed the values that have been recorded.

From the results shown the use of the theoretical prediction equations gave results which enabled the test to be carried out successfully and allowed the tests to be conducted safely.

## 5.4 Increases in Prestressing Force

Through observation of the prestressing force recorded within the external tendons by the System 5000 and the predicted value of the stress within the external tendons using theoretical predictions, it was found that the increase in the stresses within the tendons was larger than the predicted value. This increase can be assumed to be mainly from the increase in prestressing force that occurs within the tendons as the loading occurs.

This can be demonstrated by comparing the calculated predicted stresses and the recorded values from Appendix C for each test respectively.

The initial stresses within the external bars can be calculated as shown below, using a simple stress calculation:

For a circular sectioned bar, the stress in the tendon is given as,

$$\varepsilon_s = \text{Force} / \text{Cross-sectional Area}$$

$$(\varepsilon_s \text{ in MPA})$$

Therefore the initial stress  $\varepsilon_{p.ef}$ ,

$$\varepsilon_s = 160 / 415.27$$

$$\varepsilon_s = 385.3 \text{ MPa}$$

Hence, as described earlier, a prestressing force of 160 kN was induced onto the section, and using the theoretical prediction equation 3.9 the ultimate stress can be found. This equation is used to predict the maximum force that can be induced onto a section. This section must be a un-cracked or new section for the equation to perform as intended. For the purpose of the stress predictions made throughout this project, the assumption that all cracks formed within the section are closed after prestress to an extent that the section can be assumed a “new section”. Thus all predictions made were expected

to be approximate until verified by the results. This assumption has been identified as fact through all observations of the prestressing tests, where all cracks were closed. The results obtained again reassure the use of this equation, as the increase in flexural strength in both prestressing tests confirm that the cracks were closed and the section acted as a “new section”.

The ultimate stress calculation requires that the ultimate stress in the tendons are calculated by the addition of the initial prestress ( $\varepsilon_{p.ef}$ ) and the incremental stress increase under loading. The ultimate stressing calculation yields the following results:

$$\varepsilon_{pu} = 484.2 \text{ MPA}$$

Hence, with the ultimate stress calculated, the force within the tendon ( $T_p$ ) can be calculated with the rearranging of equation 3.9,

$$\text{Force} = \text{Cross-sectional Area} \times \varepsilon$$

$$\text{Force} = 201.07 \text{ kN}$$

Therefore the force within the tendon ( $T_p$ ) using the described prediction equation 3.9 from AS 3600 yields a resulting force to fail the prestressed beams in flexure as 201.07 kN. The force described is the theoretical maximum force that can the prestressed section can hold before failure, though through observation of the System 5000 outputs (Appendix C) of the maximum prestressing force measured through the loading cells gives results as shown below in Table 5.7.

The values shown below are the values of the maximum force within each prestressing tendon for the tests of Beam 2 and Beam 4, which can be seen in the columns of the System 5000 loading cells output 8 and 9.

Beam 2 (A = 1 m) Output line 8 Output line 9 130.95 kN 125.95 kN Total prestressing force of 256.9 kN

Beam 4 (A = 0.5 m) Output line 8 Output line 9 131.8 kN 127.93 kN Total prestressing force of 259.73 kN

A summary of the variance of the maximum force achieved in the prestressing tendons

Table 5.7: Recorded Values of Prestressing Force within the Prestressing Tendons

Loading Position	Total Theoretical Force (kN)	Recorded Total Force(Load Cells) (kN)	Variance (kN)
Beam 2 (A = 1 m)	201.07	256.9	55.83
Beam 4 (A = 0.5 m)	107.45	128.94	58.66

as outputted by the System 5000 results in Appendix A with the predicted ultimate force which can be seen in Table 5.7.

Therefore by implementing these recorded maximum force values in-place of the AS 3600 predicted ultimate force calculated in section 3.6 from the initial 160 kN prestressing force (where ultimate stress = initial prestress + incremental stress), an idea of how accurate the incremental increase in stress prediction can be made. This analysis is required, as the assumption of the “new section” after prestressing needs to be verified, though the large flexural increase obtained in the results confirms that the section itself acted as a “new section” already.

Using the recorded values of the total prestressing force within the tendons as shown in Table 5.7 and substituting the new  $T_p$  into the prediction equations for the prediction of the ultimate flexural strength capacity, where the results of the substitution can be show below:

Beam 2 (A = 1 m) Recorded value to fail the prestressed section in flexure, 151.46 kN  
Flexural strength predicted value of 134.32 kN to fail the prestressed section Hence, using the recorded value of  $T_p$  the force therefore to fail the prestressed section has therefore be calculated as, 150.55 kN.

Beam 4 (A = 0.5 m) Recorded value to fail the prestressed section in flexure, 128.94 kN  
Flexural strength predicted value of 107.45 kN to fail the prestressed section. Hence, using the recorded value of  $T_p$  the force therefore to fail the prestressed section has therefore be calculated as, 121.07 kN.

It can therefore be seen that using the recorded value of  $T_p$  within the prediction

Table 5.8: Recorded Value of Force versus the Predicted Force using the Recorded value of Force within the Tendons

Loading Position	predicted Force (Using recorded $T_p$ ) (kN)	Recorded Total Force (kN)	Variance (kN)
Beam 2 (A = 1 m)	150.55	151.46	0.91
Beam 4 (A = 0.5 m)	121.07	128.94	7.87

equations, a result is achieved that is very close to the recorded loading achieved to fail the prestressed sections, shown below in Table ???. Thus it can be deduced that the equation given the correct increase in prestressing force, gives an accurate prediction, though the equation itself is not applicable for cracked sections. The variance between the initial predictions and the recorded values can therefore be traced to this limitation.

These results are of a much closer accuracy than the predicted capacity for the sections achieved by the AS 3600 equation. Thus from this it may be deduced that the prediction equations ability to predict the incremental stress within the prestressing tendons is limited, as the recorded values were of a greater magnitude. Even though the sections were cracked, and then on prestressing all cracks were closed, effects on the accuracy to predict are impeded. As shown above, given the value of  $T_p$  the equations can predict the flexural strength to a high level of accuracy.

The increase in prestressing force can be simply quantified given the maximum values, though it is necessary to demonstrate the increase in prestress over the loading period of the tests. Figure 5.13 demonstrates how the prestressing force increases as the beam deflects over time,

It can be seen in Figure 5.13 that the increase is not a linear increase. This is the second order effects of the eccentricity on the prestressing bars increasing as the beam deflects causing the curved slope of the line. The second order effects have not been quantified in this project and have been assumed negligible. Figure 5.13 demonstrates that the initial prestressing force was initiated at 160 kN which then increased as the load was applied. As the loading increased, the deflection increased, which causes the increased

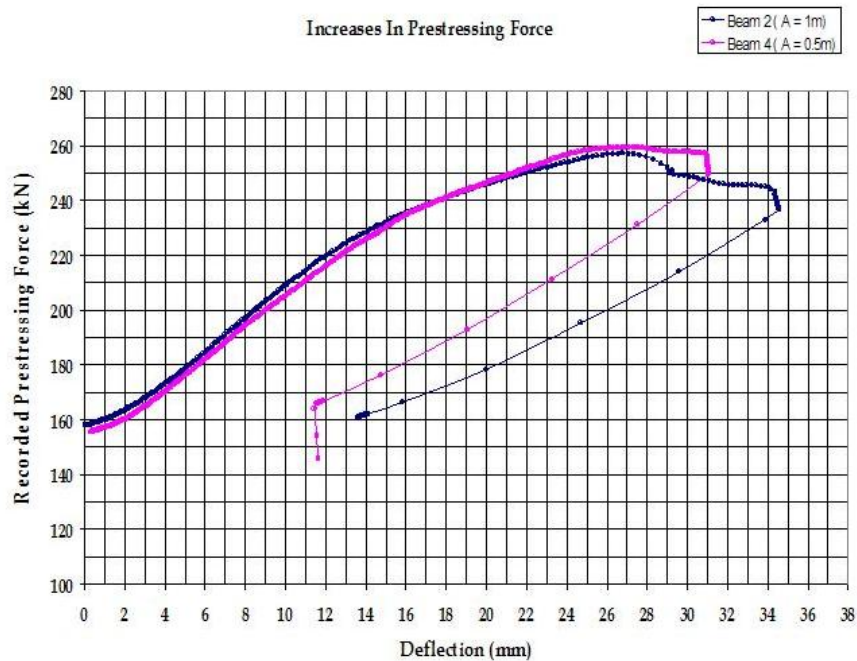


Figure 5.13: Increase in Prestressing Force

prestressing force within the tendons. The prestressing force within the tendons, as seen on the peak of the curve, achieved about a 260 kN force.

## 5.5 Conclusion

The results showed a large increase in flexural strength in the flexural beam specimens and a large reduction in deflections after prestressing. The beams all failed in a ductile fashion and failed as the design had intended. The shear cracks formed did not lead to any type of shear failure and the beams failed as any under-reinforced section is expected. Also it can be concluded from the sensitivity analysis that when the value of the force within the tendons ( $T_p$ ) was altered to the recorded value from System 5000, rather than the predicted value, the equations resulted in a value that was very much similar to the experimental results. Thus it can be concluded that external post-tensioning is a viable technique for the rehabilitation of flexural members, given that the prestressing force is large enough to close all cracks on the section.

## Chapter 6

# Conclusion

The application of external prestressing in the field of strengthening and rehabilitation of existing concrete structures is either economically feasible or a legally bound approach to solving the problem of aging and overloading of existing concrete structures. The process can be economical in the sense that the member or structure will either be replaced or rebuilt if not restored through such techniques, or legally driven given that un-safe concrete structures are bound by legislation.

### 6.1 Completion of Aims and Objectives

This project aimed to investigate the variation in flexural strength of rectangular reinforced concrete beams with the application of an external prestressing. The project also aimed to monitor the deflections and cracks formed under the two loading conditions. The major aims and objectives of this project accompanied with the outcomes of these aims are listed below:

- The aim was to develop a sound external prestressing application technique.

The external prestressing technique used was simply two external prestressing bars, which were anchored at each end via some steel plates. Both the bars and plates and all equipment were supplied by the University, thus the prestressing



technique was somewhat provided.

- To obtain the magnitude of the change in the specimens flexural strength after external prestressing.

The magnitude of the change of the flexural strengthening of the test beams was found and quantified in the results section. The increase in external prestress was found to be a 50 % and 74 % increase for the loading positions of 1 m and 0.5 m respectively.

- To observe and compare the change in the specimens deflections and crack widths.

The deflections have also been quantified throughout the results section. The results have shown that given the prestressing system, the deflections have been decreased by 63 % and 59% for the loading positions of 1 m and 0.5 m respectively.

- To compare the experimental results with the theoretical predictions.

The experimental and theoretical results were compared, and slight variances were found to exist for both the control and prestressed conditions. Various insights into why the inaccuracy has occurred have been listed. The variance of the experimental to theoretical results has been found to be 23% and 13.7% for the control beam condition, and 12.8% and 20 % for the prestressed condition for the position of 1 m and 0.5 m loading respectively.

- Discuss other unexpected outcomes of the experimental phase.

The only evident unexpected outcome that was encountered throughout the project was in-fact the difference in theoretical and experimental results. Though, section 5.4 has attempted to clarify why such differences may occur.

All major aims of this project have been achieved, with satisfactory results. A large increase in flexural capacity has been achieved with a large reduction in deflection. The overall rigidity and stiffness of the beams have been increased, though ductile failure was still observed. Not only was the strength of the section increased, but all cracks closed after prestressing.

---

## 6.2 Conclusion

To conclude this research project, it is my recommendation that the further studies be carried out on the relevant load positions, section dimensions, prestressing bar areas and prestressing forces within the system to further improve the results. From this project it can be concluded, that this style of prestressing yields very good flexural strength increases, and a large decreases in deflection given the loading positions and prestressing forces that were applied. Thus this technique proves very useful in the rehabilitation of existing flexural members in similar loading conditions. The large increase in flexural strength and effectiveness of the prestressing force to close the cracks present within the beam reinforce the effectiveness of this technique as a means to rehabilitate flexural members in service. This type of prestress could prove useful given that no crack repair methods, such as epoxy injection should not be called for to strengthen the beam. The extra rigidity and stiffness gained from the prestress will ensure that the cracks remain closed unless an overloading state is achieved. Though if the overloading is then removed, the elasticity of the system should again close all cracks.

Though this prestressing method is a more conventional method, the experimental data and results further prove that it is in-fact an effective method. This type of external prestress is limited by the fact that external bars are used for the prestressing force, thus can only be practical in shorter spans. Also the space requirements required for the jacks, and prestressing equipment to achieve the required stress can limit such a technique.

## 6.3 Recommendations for further studies

From the results of this project some recommendations for further research into certain areas of interest which have arisen are shown below:

- The effect of the secondary effect on the results

- Loading positions greater than 1m, and the effect this has on the cracking patterns, and if the shear cracks become more evident. If this loading position will induce a shear failure.
- If crack repairing techniques in-fact increase the strength of the flexural members evidently enough to support the use of these techniques in addition to the prestress.
- Further tests including reduction of the section size, the size of the prestressing bars and the prestressing force, to test if the cracks on the section still close after prestress.
- The losses in the prestressing bars over time need to be calculated or tested, so that management of the maintenance of the re-stressing of the prestress can be done accurately. Accurate re-stress ensures that the cracks will remain closed and no durability factors will influence the strength. Further study into a form of weather resistant coating on the e
- external bars may be a possibility in the near future.
- If the need rehabilitated concrete member are in future overloaded beyond the design prestress, cracking may again form and an increase in the prestressing force may be required
- A detailed study into the increase in prestressing force using outside formula, rather than using a “new section” prediction equation to predict the force of an in-fact cracked section, though assumed to be a “new section”.

# References

- Cement & of Australia, C. A. (2002), *Guide to Concrete Construction, SAA HB64*, Standards Australia.
- E. Sayed-Ahmed, H. Raid-Amr, N. S. (2004), 'Flexural strengthening of precast reinforced concrete bridge girders using bonded carbon fibre reinforced polymer strips or external post-tensioning', *Canadian Journal of Civil Engineering* **31**(3).
- for Civil Engineering, A. S. (2003), *Structural Engineering*, Standards Australia.
- H.U. Aeberhard, P. Buergi, H.-P. M. P. T. S. (2005), *External Post-Tensioning*, VSL International LTD.  
[http://www.vsl.net/downloads/VSL\\_technical\\_reports/PT\\_External.pdf](http://www.vsl.net/downloads/VSL_technical_reports/PT_External.pdf)  
current August 2005.
- Nilson, A. (1997), *Design of Concrete Structures*, 12th edn, McGraw-Hill NY.
- Nilson, A. (2004), *Design of Concrete Structures*, 13th edn, McGraw-Hill NY.
- Nilson, A. & Winter, G. (1997), *Design of Concrete Structures*, 11th edn, McGraw-Hill NY.
- P.W. Abeles, B. B.-R. (1997), *Prestressed Concrete Designer's Handbook*, 3rd edn, Viewpoint Publications, Wexham Springs.
- Rao, P. & Mathew, G. (1996), 'Behaviour of externally prestressed concrete beams with multiple deviators', *ACI Structural Journal* **93**(4).
- R.F. Warner, B.V. Rangan, A. H. K. F. (1992), *Concrete Structures*, Addison Wesley Longman, Sydney.

Appendix A

Project Specification

University of Southern Queensland

FACULTY OF ENGINEERING AND SURVEYING

**ENG 4111/4112 Research Project**  
**PROJECT SPECIFICATION**

FOR: SHAWN DAVIS

TOPIC: INVESTIGATION OF **FLEXURAL** STRENGTHENING OF CONCRETE BEAMS USING EPOXY INJECTION AND EXTERNAL PRESTRESS

SUPERVISORS: DR THIRU ARAVINTHAN

ENROLMENT: ENG 4111 - S1, D, 2005;  
ENG 4112 – S2, D, 2005

PROJECT AIM: This project aims to investigate the variation in **flexural** strength of rectangular concrete beams with the application of an epoxy and external prestressing under a constant external loading. The investigation will include the variation of the length of specimens, the influence of positioning of the loading point.

SPONSORSHIP: Faculty of Engineering and Surveying

PROGRAMME: **Issue A, 21<sup>st</sup> March 2005**

1. Research information in relation to the size of beam required given the equipment available and research into data in relation to concrete prestress and flexural failure and loading.
2. Design a specific concrete mixture, evaluating the appropriate grading and water cement ration required.
3. Design the appropriate reinforcement required in the rectangular concrete beam, and the theoretical flexural strength of the beam.
4. Design the required length for the testing specimens to give valid flexural results and inducing enough cracking to inject the epoxy.
5. Design the prestressing parameters and the theoretical increase in flexural strength after prestressing.
6. Evaluate the flexural strength variation after the epoxy injection and prestressing application.
7. Finalize the results of the variation in flexural strength of the change in strength after the application of epoxy and prestressing has been administered.

AGREED:

(Student)

(Supervisor)